PENSOFT

SENCKENBERG
world of biodiversity

Leibniz Association

A new cryptic arboreal species of the *Cyrtodactylus brevipalmatus* group (Squamata: Gekkonidae) from the uplands of western Thailand

L. Lee Grismer[1,2], Chatmongkon Suwannapoom[3], Parinya Pawangkhanant[3], Roman A. Nazarov[4], Platon V. Yushchenko[5], Mali Naiduangchan[6], Minh Duc Le[7,8,9], Vinh Quang Luu[10], Nikolay A. Poyarkov[5,11]

1 *Herpetology Laboratory, Department of Biology, La Sierra University, 4500 Riverwalk Parkway, Riverside, California 92505, USA; https://orcid.org/0000-0001-8422-3698*

2 *Department of Herpetology, San Diego Natural History Museum, PO Box 121390, San Diego, California, 92112, USA*

3 *Division of Fishery, School of Agriculture and Natural Resources, University of Phayao, Phayao, Thailand; https://orcid.org/0000-0002-3342-1464, https://orcid.org/0000-0002-0947-5729*

4 *Zoological Museum, Moscow State University, B. Nikitskaya ul. 2, Moscow 125009, Russia; https://orcid.org/0000-0002-7827-6387*

5 *Faculty of Biology, Department of Vertebrate Zoology, M. V. Lomonosov Moscow State University, Moscow 119234, Russia; https://orcid.org/0000-0003-2686-7334*

6 *Rabbit in the Moon Foundation, Suan Phueng, Ratchaburi, Thailand; https://orcid.org/0000-0003-3752-453X*

7 *Faculty of Environmental Sciences, University of Science, Vietnam National University, Hanoi, 334 Nguyen Trai Road, Hanoi, Vietnam; https://orcid.org/0000-0002-2953-2815*

8 *Central Institute for Natural Resources and Environmental Studies, Vietnam National University, Hanoi, 19 Le Thanh Tong, Hanoi, Vietnam*

9 *Department of Herpetology, American Museum of Natural History, Central Park West at 79th Street, New York, New York 10024*

10 *Faculty of Forest Resources and Environmental Management, Vietnam National University of Forestry, Xuan Mai, Chuong My, Hanoi, Vietnam; https://orcid.org/0000-0002-0634-1338*

11 *Laboratory of Tropical Ecology, Joint Russian-Vietnamese Tropical Research and Technological Center, Nghia Do, Cau Giay, Hanoi, Vietnam; https://orcid.org/0000-0002-7576-2283*

http://zoobank.org/C4C4EB21-D28B-45CD-8D9D-23EDFE37DEF2

Corresponding authors: L. Lee Grismer (lgrismer@lasierra.edu), Nikolay A. Poyarkov (n.poyarkov@gmail.com)

Academic editor Uwe Fritz | **Received** 3 October 2021 | **Accepted** 28 October 2021 | **Published** 25 November 2021

Citation: Grismer LL, Suwannapoom C, Pawangkhanant, P, Nazarov RA, Yushchenko PV, Naiduangchan M, Le MD, Luu VQ, Poyarkov NA (2021) A new cryptic arboreal species of the *Cyrtodactylus brevipalmatus* group (Squamata: Gekkonidae) from the uplands of western Thailand. Vertebrate Zoology 71 723–746. https://doi.org/10.3897/vz.71.e76069

Abstract

The first integrative taxonomic analysis of the *Cyrtodactylus brevipalmatus* group of Southeast Asia recovered two newly discovered populations from the Tenasserim Mountains in Suan Phueng District, Ratchaburi Province, Thailand as a new species described here as *C. rukhadeva* sp. nov. Based on 1397 base pairs of the mitochondrial gene NADH dehydrogenase subunit 2 (ND2), *C. rukhadeva* sp. nov. is the well-supported sister species to a clade containing three undescribed species, *C. ngati,* and *C.* cf. *interdigitalis* with a large uncorrected pairwise sequence divergence from other species in the *brevipalmatus* group ranging from 15.4–22.1%. *Cyrtodactylus elok* and *C. brevipalmatus* are recovered as poorly supported sister species and the well-supported sister lineage to the remainder of the *brevipalmatus* group. *Cyrtodactylus rukhadeva* sp. nov. is putatively diagnosable on the basis of a number of meristic characters and easily separated from the remaining species of the *brevipalmatus* group by a number of discrete morphological characters as well as its statistically significant wide separation in multivariate morphospace. The discovery of *C. rukhadeva* sp. nov. continues to underscore the unrealized herpetological diversity in the upland forests of the Tenasserim Mountains and that additional field work will undoubtedly result in the discovery of additional new species.

Key words

Bent-toed geckos, integrative taxonomy, Southeast Asia, Tenasserim Mountains

Introduction

Taxonomic partitioning of closely related, highly specialized, cryptic species has always been challenging because strong selection pressures on morphological characters can result in high degrees of parallel evolution. This is especially true for the *Cyrtodactylus brevipalmatus* group of continental Southeast Asia (Grismer 2008; Grismer et al. 2021a). Most members of this group are generally slow moving, cryptically colored species with prehensile tails (Fig. 1) and partially webbed digits and spend most of their time above ground level—often in dense vegetation, beneath exfoliating bark, in root tangles, or within tree trunk crevices (Smith 1923; Ulber 1993; Grismer 2011; Nurngsomsri et al. 2014; Grismer et al. 2021b). The group currently contains four nominal species and at least three undescribed species (Chomdej et al. 2021; Grismer et al. 2021a) that range from northwestern Vietnam, Laos and Thailand, then southward along the Thai-Malay Peninsula to southern Peninsular Malaysia (Fig. 1). A recent molecular phylogeny of the group recovered the new species, *C. ngati* Le, Sitthivong, Tran, Grismer, Nguyen, Le, Ziegler & Luu from northwestern Vietnam (Le et al. 2021), as the sister species of *C. interdigitalis* Ulber of Thailand and Laos (Ulber 1993). However, this study did not have sufficient material to address many of the taxonomic issues surrounding the *brevipalmatus* group and the genetic sample of *C. interdigitalis* (LSUHC 11006) is of unknown provenance. In the most recent taxonomic study, Grismer (2008) noted a number of errors and misinterpretations in the literature based on misidentifications between *C. interdigitalis* and *C. brevipalmatus* Smith (Smith, 1923, 1930, 1935; Welch 1990; Ulber 1993; Manthey and Grossmann 1997; Nabhitabhata et al. 2004). These errors stemmed from the fact that these two species are extremely similar in morphology and color pattern, and if not examined carefully across a broad range of characters, are easily confused with one another. The discovery of two new populations of the *brevipalmatus* group from Suan Phueng District, Ratchaburi Province in the Tenasserim Mountains of western Thailand within the currently proposed range of *C. brevipalmatus* (Grismer 2008), prompted us to initiate the first integrative taxonomic analysis of the group. To do so, we examined a suite of morphometric and meristic characters from specimens representing three of the four nominal species combined with a molecular phylogenetic analysis using the mitochondrial gene NADH dehydrogenase subunit 2 (ND2). Our analyses confirmed the specific recognition of *C. brevipalmatus* from the type locality, *C. elok* Dring, and *C. ngati* from its type localities, and that the newly discovered populations from Suan Phueng District comprise a new species described below. Furthermore, we provide molecular evidence strongly indicating that *C. brevipalmatus* does not range north of the Isthmus of Kra on the Thai-Malay Peninsula and reports of this species from western Thailand (Smith 1935; Welch et al. 1990; Ulber 1993; Manthey and Grossmann 1997; Nabhitabhata et al. 2004; Grismer 2008; Ellis and Pauwels 2012; Pauwels and Chan-ard 2014) comprise perhaps, as many as three undescribed species. We were not, however, able to examine specimens or acquire sequence data from *C. interdigitalis* from the type locality in Nam Nao National Park, Petchabun Province, Thailand. Therefore, populations from Laos and Thailand outside the type locality generally referred to as *C. interdigitalis* (e.g. Manthey and Grossmann 1997; Cox et al. 1998; Chan-ard et al. 1999, 2015; Stuart 1999; Nabhitabhata and Chan-ard 2005; Ellis and Pauwels 2012; Nurngsomsri et al. 2014; Grismer and Davis 2018; Chomej et al. 2021) are treated here as *C.* cf. *interdigitalis* pending further investigations.

Methods

Sampling

Specimens were collected in Suan Phueng District, Ratchaburi Province, Thailand by Parinya Pawangkhanant, Platon V. Yushchenko, Mali Naiduangchan, Chatmongkon Suwannapoom, and Nikolay A. Poyarkov during several field surveys in 2019 (Fig. 2). Geographic coordinates and elevations were obtained using a Garmin GPSMAP 60CSx and recorded in WGS 84 datum. Specimens were collected by hand, anaesthetized and euthanized with 20% benzocaine solution, femoral muscle or liver tissue samples removed, and then fixed in 10% buffered formalin before preserving in 70% ethanol. The tissue samples were stored in 95% ethanol. Specimens and tissues were subsequently deposited in the herpetological collections of the School of Agriculture and Natural Resources, University of Phayao (AUP, Phayao, Thailand) and of the Zoological Museum of Moscow University (ZMMU, Moscow, Russia).

Specimen collection and animal use protocols were approved by the Institutional Ethical Committee of Animal Experimentation of the University of Phayao, Phayao, Thailand (certificate number UP-AE61-01-04-022, issued to Chatmongkon Suwannapoom) and were strictly complacent with the ethical conditions of the Thailand Animal Welfare Act. Field work, including collection of animals in the field and specimen exportation, was autho-

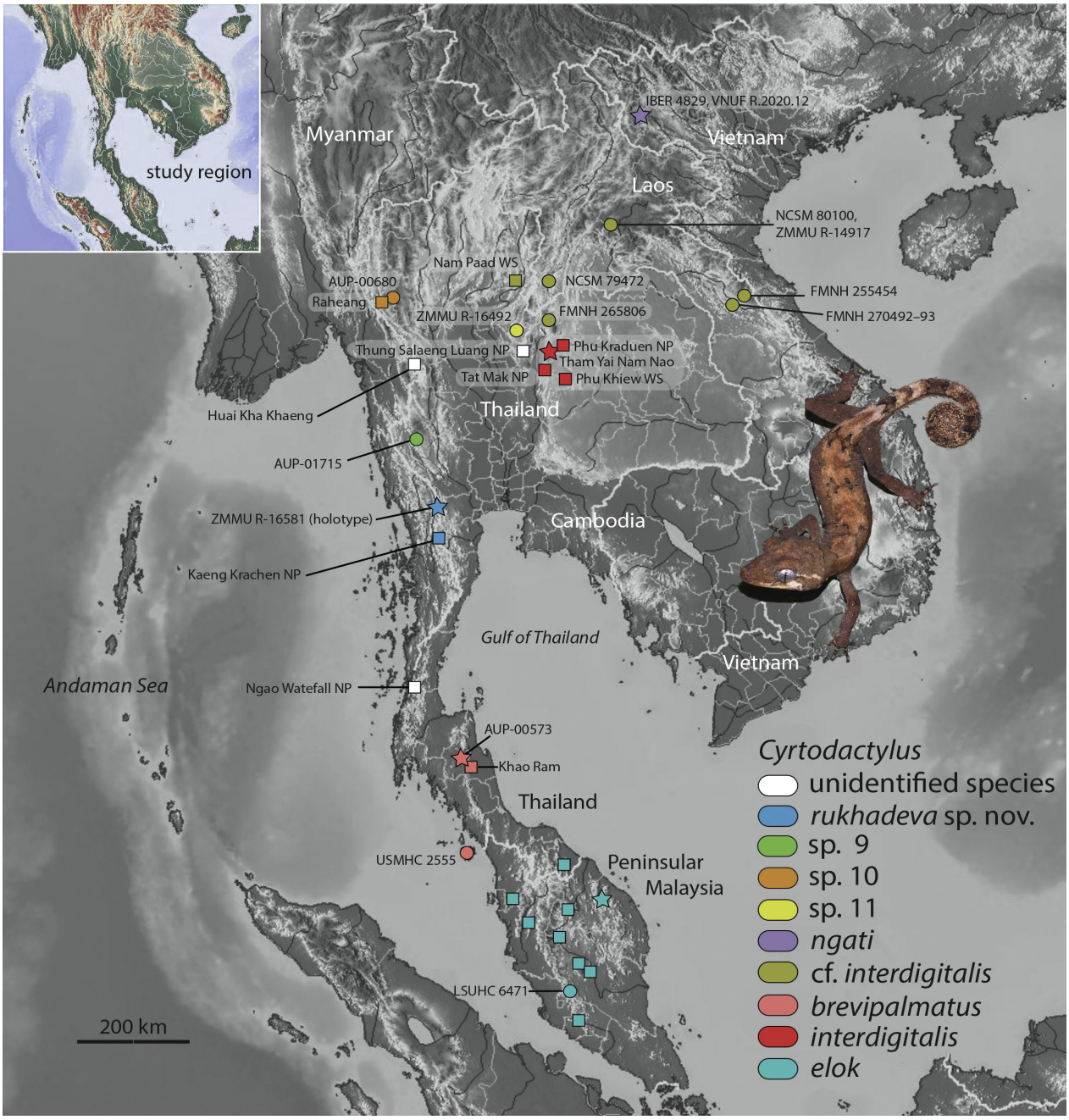

Figure 1. Distribution of the species of the *Cyrtodactylus brevipalmatus* group. Stars = type localities and squares refer to literature records. White squares denote unexamined specimens of uncertain taxonomic status. Localities with specimen numbers denote individuals in the phylogeny (Fig. 2). No topotypic material (red) from the western Phetchabun massif was examined. NP = National Park and WS = Wildlife Sanctuary.

rized by the Institute of Animals for Scientific Purpose Development (IAD), Bangkok, Thailand (permit numbers U1-01205-2558 and UP-AE59-01-04-0022, issued to Chatmongkon Suwannapoom).

Morphological data and analyses

Morphological data included both meristic and morphometric characters. Measurements were taken on the left side of the body when possible to the nearest 0.1 mm using dial calipers under dissecting microscope following Murdoch et al. (2019). Measurements taken were: snout-vent length (SVL), taken from the tip of the snout to the vent; tail length (TL), taken from the vent to the tip of the tail, original or partially regenerated; tail width (TW), taken at the base of the tail immediately posterior to the postcloacal swelling; humeral length (HumL), taken from the medial end of the humerus at its insertion point in the glenoid fossa to the distal margin of the elbow while flexed 90°; forearm length (ForL), taken on the ventral surface from the posterior margin of the elbow while flexed 90° to the inflection of the flexed wrist; femur length (FemL), taken from the medial end of the femur at its insertion point in the acetabulum to the distal margin of the knee while flexed 90°; tibia length (TibL),

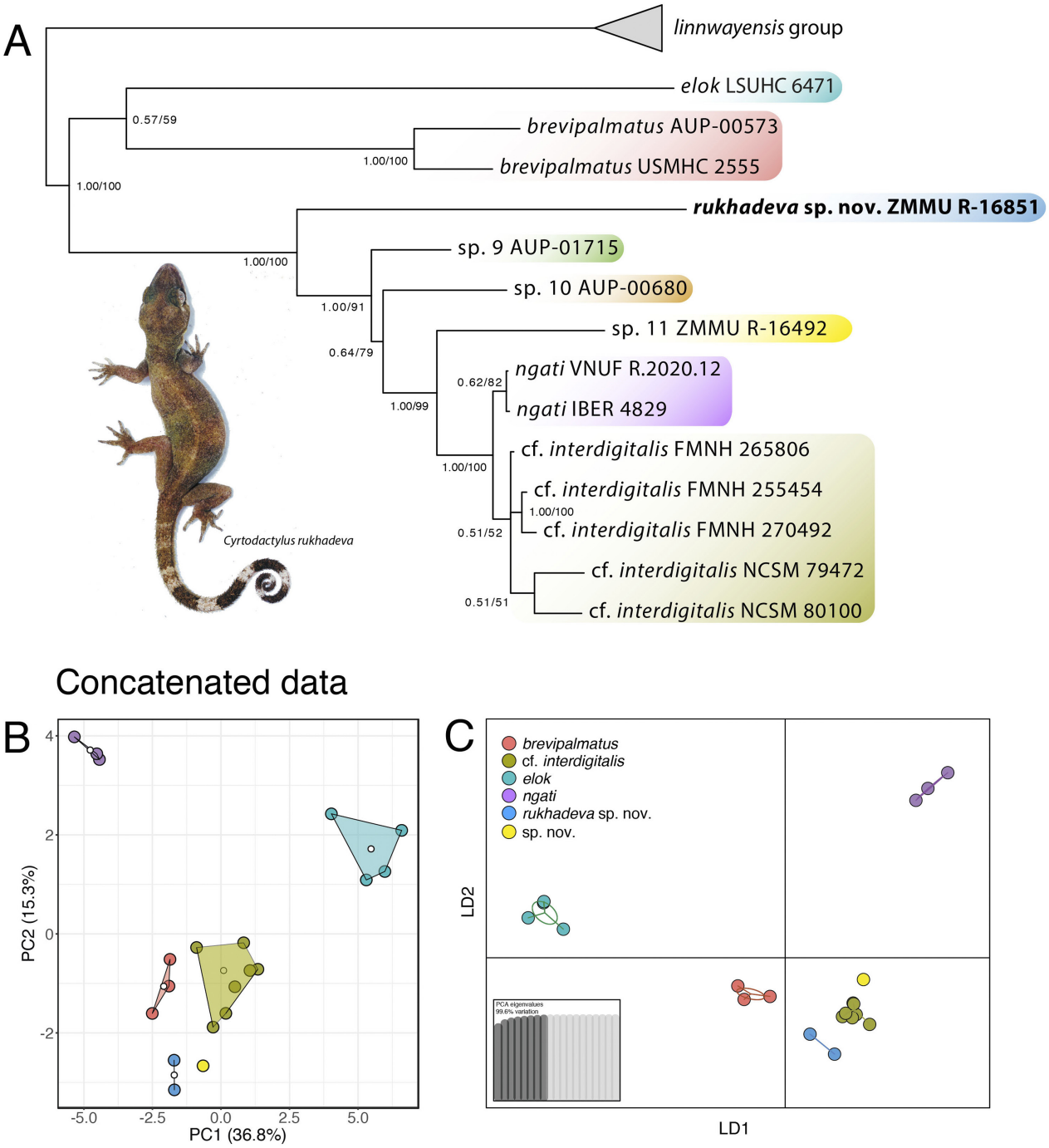

Figure 2. A. Bayesian phylogeny of the *Cyrtodactylus brevipalmatus* group based on 1397 base pairs of ND2 with BBP and UFB nodal support values, respectively at the nodes. B. PCA based on concatenated meristic and adjusted morphometric data. C. DAPC based on concatenated meristic and adjusted morphometric data.

taken on the ventral surface from the posterior surface of the knee while flexed 90° to the base of the heel; axilla to groin length (AG), taken from the posterior margin of the forelimb at its insertion point on the body to the anterior margin of the hind limb at its insertion point on the body; head length (HL), the distance from the posterior margin of the retroarticular process of the lower jaw to the tip of the snout; head width (HW), measured at the angle of the jaws; head depth (HD), the maximum height of head measured from the occiput to base of the lower jaw; eye diameter (ED), the greatest horizontal diameter of the eye-ball; eye to ear distance (EE), measured from the anterior edge of the ear opening to the posterior edge of the bony orbit; eye to snout distance or snout length (ES), measured from anteriormost margin of the bony orbit to the tip of snout; eye to nostril distance (EN), measured from the anterior margin of the bony orbit to the posterior margin of the external nares; interorbital distance (IO), measured between the dorsal-most edges of the bony orbits; internarial distance (IN), measured between the nares across the rostrum; and ear length (EL), greatest oblique length across the auditory meatus.

Meristic characters evaluated were the number of supralabial scales (SL), counted from the largest scale im-

mediately below the middle of the eyeball to the rostral scale; infralabial scales (IL), counted from the mental to the termination of enlarged scales just after the upturn of the mouth; the number of paravertebral tubercles (PVT), between limb insertions counted in a straight line immediately left of the vertebral column; the number of longitudinal rows of body tubercles (LRT), counted transversely across the center of the dorsum from one ventrolateral fold to the other; the number of longitudinal rows of ventral scales (VS,) counted transversely across the center of the abdomen from one ventrolateral fold to the other; the number of transverse rows of ventral scales (VSM), counted along the midline of the body from the postmentals to the cloacal opening; the number of expanded subdigital lamellae on the fourth toe proximal to the digital inflection (TL4E), counted from the base of the first phalanx where it contacts the body of the foot to the largest scale on the digital inflection—the large contiguous scales on the palmar and plantar surfaces were not counted; the number of small, generally unmodified subdigital lamellae distal to the digital inflection on the fourth toe (TL4U), counted from the digital inflection to the claw including the claw sheath (see Murdoch et al. 2019: Fig. 2); the total number of subdigital lamellae (TL4T) beneath the fourth toe (i.e. TL4E + TL4U = TL4T); the number of expanded subdigital lamellae on the fourth finger proximal to the digital inflection (FL4E) counted from the base of the first phalanx where it contacts the body of the foot to the largest scale on the digital inflection—the large contiguous scales on the palmar and plantar surfaces were not counted; the number of small, generally unmodified subdigital lamellae distal to the digital inflection on the fourth finger (FL4U) counted from the digital inflection to the claw including the claw sheath (see Murdoch et al. 2019: Fig. 2); the total number of subdigital lamellae (FL4T) beneath the fourth toe (i.e. FL4E + FL4U = FL4T); the total number of enlarged femoral scales (FS) from each thigh combined as a single metric; the number of enlarged precloacal scales (PCS); the number of precloacal pores in (PP) in males; the number of femoral pores in (FP) in males; the number of rows of post-precloacal scales (PPS) on the midline between the enlarged precloacal scales and the vent; and the number of dark body bands (BB) between the nuchal loop (the dark band running from eye to eye across the nape) and the hind limb insertions. Other morphological characters evaluated were the presence or absence of paravertebral tubercles, enlarged femoral scales, small tubercles on the forelimbs and flanks, paried or single enlarged subcaudal scales; large or small dorsolateral and ventrolateral caudal fringe scales (i.e. fringes), and the cross-section of the tail round or more square in shape.

Small sample sizes (n=1–3) from some of the populations/species precluded meaningful statistical analyses. However, the morphospatial clustering among the species for the meristic, morphometric, and concatenated datasets was visualized using principal component analysis (PCA) and discriminant analysis of principal components (DAPC) from the ADEGENET package in R (Jombart et al. 2010). We analyzed each data type (i.e. meristic and morphometric) separately in order to visualize the contribution of each to the variation in the group and then we concatenated the data types to visualize their overall contribution to the variation of the group. Previous studies have demonstrated that concatenated data sets generally outperform single data sets in capturing the overall morphological variation among closely related species (Grismer et al. 2018, 2020a, 2021).

Morphometric characters analyzed were SVL, AG, HumL, ForL, FemL, TibL, HL, HW, HD, ED, EE, EN, IO, EL, and IN. To remove potential effects of allometry in the morphometric dataset, size was normalized using the following equation: $X_{adj}=\log(X)-\beta[\log(SVL)-\log(SVL_{mean})]$, where X_{adj}=adjusted value; X=measured value; β=unstandardized regression coefficient for each population; and SVL_{mean}=overall average SVL of all populations (Thorpe 1975, 1983; Turan 1999; Lleonart et al. 2000, accessible in the R package *GroupStruct* (available at https://github.com/chankinonn/GroupStruct). The morphometrics of each species were normalized separately and then concatenated so as not to conflate intra- with interspecific variation (Reist 1986). All data were scaled to their standard deviation to insure they were analyzed on the basis of correlation and not covariance.

Meristic characters analyzed were SL, IL, LRT, VS, VSM, TL4E, TL4U. TL4T, FL4E, FL4U, FL4T, PCS, PPS, and BB. Paravertebral tubercles (PVT), enlarged femoral scales (FS) were not included due to their absence in *Cyrtodactylus elok.* Precloacal and femoral pores were also omitted due to their absence in females. For corroboration of the PCA, a discriminant analysis of principal components (DAPC) was performed on the same data sets. DAPC is a supervised analysis that relies on scaled data calculated from its own internal PCA as a prior step to ensure that variables analyzed are not correlated and number fewer than the sample size. Dimension reduction of the DAPC prior to plotting, is accomplished by retaining the first set of PCs that account for 90–99% of the variation in the data set (Jombart and Collins 2015) as determined from a scree plot generated as part of the analysis. The ranges, means, medians, and 50% quartiles were visualized using boxplots for the meristic data and violin plots with embedded boxplots for the mensual data. All analyses were performed in R [v3.4.3].

Genetic data

For the molecular phylogenetic analyses, we extracted the total genomic DNA from ethanol-preserved femoral muscle tissue of six specimens of the new Thai populations using standard phenol-chloroform-proteinase K extraction procedures with consequent isopropanol precipitation, for a final concentration of about 1 mg/ml (protocols followed Hillis et al. (1996) and Sambrook and David (2001)). We visualized the isolated total genomic DNA in agarose electrophoresis in the presence of ethidium bromide. We measured the concentration of total DNA in 1 μl using NanoDrop 2000 (Thermo Scientific), and consequently adjusted to ca. 100 ng DNA/μL.

We amplified mtDNA fragments of ND2 and its flanking tRNAs using a double-stranded Polymerase Chain Reaction (PCR) to obtain a 1397 base pairs under the following conditions: 1.0 µl genomic DNA (10–30 µg), 1.0 µl light strand primer (concentration 10 µM), 1.0 µl heavy strand primer (concentration 10 µM), 15 µl Master Mix 2x (CWBIO, China), and 12 µl ultra-pure H2O. PCR reactions were executed on Bio-Rad T100™ gradient thermocycler under the following conditions: initial denaturation at 94 °C for 5 min, followed by a second denaturation at 94 °C for 60 s, annealing at 58 °C for 60 s, followed by a cycle extension at 72 °C for 60 s, for 35 cycles with the final extension step 72 °C for 10 min. For amplification of the full ND2 gene with parts of adjacent tRNAs we used the NADH2-Metf6 (5'-AAGCTTTCGGGCCCATACC-3') and CO1H (5'-AGRGTGCCAATGTCTTTGTGRTT-3') primers following Macey et al (1997).

PCR products were loaded onto 1.5% agarose gels in the presence of ethidium bromide and visualized in agarose electrophoresis. When distinct bands were produced, we purified the PCR products using 2 µl of a 1:4 dilution of ExoSapIt (Amersham) per 5 µl of PCR product prior to cycle sequencing. A 10 µl sequencing reaction included 2 µL of template, 2.5 µl of sequencing buffer, 0.8 µl of 10 pMol primer, 0.4 µl of BigDye Terminator version 3.1 Sequencing Standard (Applied Biosystems) and 4.2 µl of water. The cyclesequencing used 35 cycles of 10 sec at 96°C, 10 sec at 50°C and 4 min at 60°C. We purified the cycle sequencing products by ethanol precipitation. We carried out sequence data collection and visualization on an ABI 3730xl Automated Sequencer (Applied Biosystems).

Phylogenetic analyses

Ingroup samples consisted of 14 individuals of the *brevipalmatus* group representing three nominal species including a sample from one of the new populations in Suan Phueng District plus five individuals of *Cyrtodactylus* cf. *interdigitalis* from Thailand and Laos. Four species of the *linnwayensis* group were used to root the tree following Grismer et al. (2021b). Sequence data for some specimens were acquired from GenBank and newly generated sequences were deposited in GenBank (Table 1).

Maximum Likelihood (ML) and Bayesian Inference (BI) were used to estimate phylogenetic trees. Best-fit models of evolution determined in IQ-TREE (Nguyen et al. 2015) using the Bayesian information criterion (BIC) implemented in ModelFinder (Kalyaanamoorthy et al. 2017) indicated that TNe+I+G4 was the best-fit model of evolution for the tRNAs and HKY+F+G4, TIM3+F+G4, and TPM3u+F+I+G4 were the best models of evolution for codon positions 1, 2, and 3, respectively. The ML analysis was performed using the IQ-TREE webserver (Trifinopoulos et al. 2016) with 1000 bootstrap pseudoreplicates using the ultrafast bootstrap (UFB) analysis (Minh et al. 2013; Hoang et al. 2018). The BI analysis was performed on CIPRES Science Gateway (Miller et al. 2010) using MrBayes v3.2.4 (Ronquist et al. 2012). Two independent runs were performed using Metropolis-coupled Markov Chain Monte Carlo (MCMCMC), each with four chains: three hot and one cold. The MCMCMC chains were run for 15,000,000 generations with the cold chain sampled every 1500 generations and the first 10% of each run being discarded as burn-in. The posterior distribution of trees from each run was summarized using the sumt function in MrBayes v3.2.4 (Ronquist et al. 2012). Stationarity was checked with Tracer v1.7 (Rambaut et al. 2018) to be sure effective sample sizes (ESS) for all parameters were well above 200. We considered Bayesian posterior probabilities (BPP) of 0.95 and above and ultrafast bootstrap support values (UFB) of 95 and above as an indication of strong nodal support (Huelsenbeck et al. 2001; Minh et al. 2013). Uncorrected pairwise sequence divergences (p-distance) were calculated in MEGA 7 (Kumar et al. 2016) using the complete deletion option to remove gaps and missing data from the alignment prior to analysis.

Results

Phylogenetic data

The ML and BI analyses recovered trees with identical topologies (Fig. 2A). *Cyrtodactylus elok* and *C. brevipalmatus* of the Thai-Malay Peninsula were recovered as poorly supported sister species (BPP 0.57/UFB 59) and the strongly supported (1.00/100) sister lineage to a strongly supported clade (1.00/100) containing the remaining taxa. Within that clade, the individual of the new population from Suan Phueng District was recovered as the sister lineage to a monophyletic group bearing the phylogenetic sequence of sp. 9, sp. 10, sp. 11, and terminating with the strongly supported (1.00/100) sister species *C. ngati* and *C.* cf. *interdigitalis.* Support values for these nodes in are shown in Figure 2A. The phylogenetic analyses strongly supported the recognition of the Suan Phueng population as a new species, which bears a 15.4–22.1% uncorrected pairwise sequence divergence from the other species in the *brevipalmatus* group (Table 2). The phylogenetic analyses also supported the separate species status of sp. 9 and sp. 10 as previously recovered by Chomdej et al. (2021).

The phylogeny indicates species recognition for ZMMU R-16492 from Phu Hin Rong Kla National Park, Phitsanulok Province, Thailand (Fig. 1; referred to here as sp. 11) in that it is recovered as the sister species to the strongly supported (1.00/99) lineage comprised of *C. ngati* and *C.* cf. *interdigitalis* (Fig. 2). Although the locality of ZMMU R-16492 at 1147 m in elevation is only 45 km to the northwest of the type locality of *C. interdigitalis* at 700 m in Nam Nao National Park, Petchabun Province (Ulber 1993), these upland sites are separated by a 20 km wide low-lying river basin of 136 m in elevation at its lowest point with no intervening hilly terrain

Table 1. Specimens, locality, and GenBank accession numbers of specimens used in the phylogenetic analyses.

Species/specimens	**Locality**	**GenBank no.**
outgroup		
Cyrtodactylus linnwayensis LSUHC 12970	Yae Htuck Cave, Linn-Way Village, 13.3 km north-east of Ywangan, Taunggyi District, Shan State, Myanmar	MF872281
C. shwetaungorum LSUHC 2935	5.0 km north of Pyinyaung Village at the Apache Cement factory mining site, Mandalay Region.	MF872349
C. pinlaungensis LSUHC 14278	Pinlaung Town, Pinlaung Township, Pa-O District, Shan State, Myanmar.	MN030632
C. ywanganensis LSUHC 13711	2.7 km southwest of Ywangan, Ywangan Township, Taunggyi District, Shan State, Myanmar	MH607608
ingroup		
C. brevipalmatus AUP-00573	Khao Ram Mt., Nakhon Si Thammarat Province, Thailand	OK6263193
C. brevipalmatus USMHC 2555	Gunung Raya, Pulau Langkawi, Kedah, West Malaysia	OK6263194
cf. *interdigitalis* FMNH 265806	Phu Luang Wildlife Sanctuary, Nam San Noi River, Loei Province, Thailand	JX51947
cf. *interdigitalis* FMNH 255454	Phou Hin Poun National Biodiversity Conservation Area, Laos	JQ889181
cf. *interdigitalis* FMNH 270492	Phou Hin Poun National Biodiversity Conservation Area, Laos	OK6263195
cf. *interdigitalis* NCSM 79472	Ban Pha Liep, Houay Liep Stream, Xaignabouli Province, Laos	OK6263196
cf. *interdigitalis* NCSM 80100	Houay Wan Stream, tributary of Nam Pha River, Vientiane Province, Laos	OK6263197
C. elok LSUHC 6471	Negeri Sembilan, West Malaysia	JQ889180
C. ngati VNUF R.2020.12	Karst forest near Pa Thom Cave, Pa Xa Lao Village, Pa Thom Commune, Dien Bien District, Dien Bien Province, Vietnam	OK626319
C. ngati 3219 IBER 4829	Karst forest near Pa Thom Cave, Pa Xa Lao Village, Pa Thom Commune, Dien Bien District, Dien Bien Province, Vietnam	OK6263198
C. rukhadeva sp. nov. ZMMU R-16851 (holotype)	Khao Laem Mountain, Suan Phueng District, Ratchaburi Province, Thailand	OK62631920
C. sp. 9 AUP-01715	Thong Pha Phum National Park, Thong Pha Phum District, Kanchanaburi Province, Thailand	MT468909
C. sp. 10 AUP-00680	as Chao Doi Waterfall, Mae Moei National Park, Tha Song Yang District	MT468902
C. sp. nov. ZMMU R-16492	Phu Hin Rong Kla National Park, Phitsanulok, Petchabun Province, Thailand,	MW792061

Table 2. Uncorrected pairwise sequence divergence of ND2 and the flanking tRNAs among the individuals of clade 1 of the *Cyrtodactylus brevipalmatus* species group. Highlighted cells denote sequence divergence of each species from *C. rukhadeva* sp. nov.

Specimens	**1**	**2**	**3**	**4**	**5**	**6**	**7**	**8**	**9**	**10**	**11**	**12**	**13**
1. *brevipalmatus* USMHC2555													
2. *brevipalmatus* AUP-00573	0.063												
3. cf. *interdigitalis* FMNH255454	0.204	0.206											
4. cf. *interdigitalis* FMNH265806	0.207	0.206	0.009										
5. cf. *interdigitalis* FMNH270492	0.204	0.208	0.008	0.014									
6. cf. *interdigitalis* NCSM79472	0.211	0.211	0.036	0.030	0.041								
7. cf. *interdigitalis* NCSM80100	0.207	0.216	0.037	0.033	0.042	0.045							
8. *elok* JQ889180	0.198	0.206	0.212	0.210	0.213	0.226	0.213						
9. *ngati* VNUF R.2020.12	0.207	0.206	0.010	0.001	0.015	0.031	0.035	0.208					
10. *ngtai* IBER 4829	0.207	0.206	0.010	0.001	0.015	0.031	0.035	0.208	0.000				
11. *rukhadeva* sp. nov. ZMMU R-16851	0.206	0.213	0.161	0.156	0.165	0.158	0.161	0.221	0.154	0.154			
12. sp.10_AUP-00680	0.188	0.198	0.099	0.099	0.103	0.093	0.107	0.219	0.100	0.100	0.149		
13. sp.9 AUP-01715	0.195	0.202	0.091	0.084	0.095	0.080	0.094	0.219	0.082	0.082	0.138	0.078	
14. sp. nov. HLM0320	0.197	0.203	0.084	0.080	0.085	0.073	0.089	0.221	0.081	0.081	0.162	0.103	0.089

(Fig. 1). Similarly, *C.* cf. *interdigitalis* FMNH 265806 from the Phu Luang Wildlife Sanctuary occurs at 850 m in elevation and is 65 km north of the type locality of *C. interdigitalis* but separated from it by an approximately15 km wide low-lying river basin at approximately 200 m at its lowest point. ZMMU R-16492 lies 50 km to the south-west of FMNH 265806 and it too is separated by a low-lying river basins. Given the close geographic proximity of these three topographically separated upland localities and the fact that ZMMU R-16492 and FMNH 265806 are not each other's closest relatives, makes it premature to consider either as conspecific with *C. interdigitalis* in the

absence of genetic data from the type locality or at least morphological data from the type series. Both options are currently being explored.

Although the monophyly of *Cyrtodactylus* cf. *interdigitalis* and *C. ngati* is strongly supported, the monophyly of each of them is not. Although it is difficult to conceive that *C. ngati* would not be monophyletic given that all specimens were found on the same karst formation approximately 200 km north of the nearest population of *C.*cf. *interdigitalis* (Fig.1)*,* nodal support for its monophyly is only 0.62/82. That of *C.* cf. *interdigitalis* ranging from northern Laos to central Thailand is even less—0.51/52. If these nodes were collapsed on the basis of low support values, it would be phylogenetically conceivable to consider *C. ngati* and *C.* cf. *interdigitalis* as conspecific. However, these two species are trenchantly different in morphology (see below) and again, the absence of any data from the type locality of *C. interdigitalis,* makes any taxonomic proposal premature.

Multivariate data

The PCA of the concatenated meristic and adjusted morphometric data sets corroborated the phylogenetic analyses in that the Suan Phueng individuals are not embedded within the cluster of any other species along the combined ordination of principal component (PC) 1 and PC2 (Fig. 2B). PC1 accounted for 36.8% of the variation and loaded most heavily for AG, FemL, HW, HD, EL and FS. PC2 accounted for 15.3% of the variation and loaded most heavily for FL4T and BB (Table 3). These results were mirrored in the DAPC of the concatenated data (Fig. 2C). The PCA of the morphometric data also recovered separation of the Suan Phueng individuals along both axes but very close to *C.* cf. *interdigitalis*. In the DAPC, however, the Suan Phueng individuals were within the 66% confidence ellipsoid of *C.* cf. *interdigitalis* (Fig. 3). PC1 accounted for 50.2% of the variation and loaded most heavily for ES, HD, AG, FemL, and HL (Fig. 4) and PC2 accounted for an additional 16.2% of the variation, loading most heavily for IO, IN, and EN. The meristic data also recovered separation of the Suan Phueng populations along the combined axes in the PCA and DAPC but again, closest to *C.* cf. *interdigitslis* (Fig. 5). PC1 accounted for 35.0% of the variation and loaded most heavily for AG, FemL, HW, HD, EL and FS (Fig. 6) and PC2 accounted for 20.1% of the variation, loading most heavily for FL4E, TL4T, and BB.

Taxonomy

Based on the phylogenetic relationships, PCA, DAPC, and several discrete morphological differences between the Suan Phueng individuals and all other species of the *brevipalmatus* group (see comparisons below and Table 4), we hypothesize that they comprise a discretely diagnosable lineage that is not reticulating with any other lineage and as such, should be accorded species status.

Cyrtodactylus rukhadeva sp. nov.

http://zoobank.org/B979D28D-D18F-4B8A-A071-062904D4-91CC

Figures 7, 8
Suggested common name: tree spirit bent-toed gecko

Cyrtodactylus brevipalmatus Ulber 1993:198 (partim).

Holotype. Adult male ZMMU R-16851 (field tag NAP-09743, tissue sample ID HLM0372) from Thailand, Ratchaburi Province, Suan Phueng District, Khao Laem Mountain (13.53846N, 99.20071E, elevation 994 m a.s.l.), collected by Platon V. Yushchenko and Kawin Jiaranaisakul on 19 June 2019.

Paratype. Adult female ZMMU R-16852 (field tag NAP-09744) from Thailand, Ratchaburi Province, Suan Phueng District, Hoop Phai Tong (3.56210N, 99.20670E, elevation 593 m a.s.l.), collected by Platon Yushchenko on 11 July 2019.

Diagnosis. *Cyrtodactylus rukhadeva* **sp. nov.** can be separated from all other species of the *brevipalmatus* group by having 9–11 supralabials, 10 or 11 infralabials, 27–30 paravertebral tubercles, 19 or 20 rows of longitudinally arranged tubercles, 34–43 transverse rows of ventrals, 152–154 longitudinal rows of ventrals, nine expanded subdigital lamellae on the fourth toe, 11 unexpanded subdigital lamellae on the fourth toe, 18–20 total subdigital lamellae on the fourth toe, eight or nine expanded subdigital lamellae on the fourth finger, nine or 10 unexpanded subdigital lamellae on the fourth finger, 17–19 total subdigital lamellae on the fourth finger, 16–17 enlarged femorals, 20 femoral pores in the male; 17 precloacal pores in the male; 13–17 enlarged precloacals; 16 post-precloacals; enlarged femorals and enlarged precloacals not continuous; proximal femorals not less than one-half the size of the distal femorals; small tubercles on forelimbs and flanks; small dorsolateral caudal tubercles and ventrolateral caudal fringe; paired enlarged subcaudals; and maximum SVL 79.4 mm (Tables 1, 4).

Description of holotype. (Figs. 7 and 8) Adult male SVL 74.9 mm; head moderate in length (HL/SVL 0.27), width (HW/HL 0.72), depth (HD/HL 0.46), distinct from neck, triangular in dorsal profile; lores concave slightly anteriorly, weakly inflated posteriorly; prefrontal region slightly concave; canthus rostralis rounded; snout elongate (ES/HL 0.41), rounded in dorsal profile; eye large (ED/HL 0.23); ear opening round, small; eye to ear distance greater than diameter of eye; rostral rectangular, partially divided dorsally by inverted Y-shaped furrow, bordered posteriorly by large left and right supranasals and one small azygous internasal, bordered laterally by first supralabials; external nares bordered anteriorly by rostral, dorsally by large supranasal, posteriorly by two smaller postnasals, bordered ventrally by first supralabial; 11(R,L) rectangular supralabials extending to below

Table 3. Summary statistics and principal component analysis scores for meristic characters of the *Cyrtodactylus brevipalmatus* group. Abbreviations are listed in the Materials and methods.

	PC1	PC2	PC3	PC4	PC5	PC6	PC7	PC8	PC9	PC10	PC11	PC12	PC13	PC14	PC15	PC16	PC17	PC18	PC19	PC20
Standard deviation	3.37678	2.18155	1.99271	1.64085	1.45155	1.13826	1.04771	0.93851	0.73481	0.70743	0.61796	0.60385	0.58611	0.43373	0.39849	0.34554	0.29144	0.26788	0.20076	0.00000
Proportion of variance	0.36783	0.15352	0.12809	0.08685	0.06797	0.04179	0.03541	0.02841	0.01742	0.01614	0.01232	0.01176	0.01108	0.00607	0.00512	0.00385	0.00274	0.00231	0.00130	0.00000
Cumulative proportion	0.36783	0.52135	0.64944	0.73629	0.80426	0.84606	0.88147	0.90988	0.92730	0.94344	0.95576	0.96752	0.97860	0.98467	0.98979	0.99365	0.99639	0.99870	1.00000	1.00000
Eigenvalue	11.40267	4.75917	3.97090	2.69239	2.10699	1.29563	1.09769	0.88081	0.53995	0.50045	0.38188	0.36463	0.34353	0.18812	0.15879	0.11940	0.08494	0.07176	0.04030	0.00000
SVL	0.20628	-0.04996	-0.17415	-0.09992	0.03167	0.25041	0.05253	-0.16520	-0.26305	0.22777	-0.36743	-0.02063	0.51823	0.39601	-0.14241	-0.12335	0.11625	0.17481	-0.02697	0.07148
AG	0.24702	-0.16326	-0.08996	0.05228	0.00719	0.04851	0.19758	-0.01491	0.29786	-0.07886	0.02223	-0.19785	-0.03556	0.06766	-0.28079	-0.08702	-0.27332	-0.26654	-0.02473	0.27942
HumL	-0.06032	-0.17954	0.11082	0.16587	-0.47728	0.28293	0.17566	-0.08457	-0.11561	-0.25461	-0.09271	0.01917	-0.07985	-0.07157	-0.13192	-0.19130	-0.22824	-0.08847	0.03658	-0.08768
ForL	0.20569	0.22709	-0.01031	0.22494	0.00049	-0.00837	0.18914	-0.21424	-0.06570	-0.02972	0.04239	0.01063	-0.12218	0.19459	0.40970	-0.05789	-0.22634	0.25154	0.31474	0.05628
FemL	0.23677	-0.10435	-0.13808	-0.02734	-0.09507	-0.12834	0.21825	-0.31133	-0.01135	-0.00611	0.11318	0.06052	0.06540	-0.37638	0.14137	0.29835	0.18797	0.09963	0.17587	-0.14032
TibL	0.22379	0.15079	-0.01240	0.22463	0.01845	-0.02043	0.18028	-0.27049	0.17476	-0.25700	0.00942	0.05390	0.20212	-0.19451	-0.19844	-0.08157	0.03322	0.03740	-0.30919	0.07693
HL	0.20935	0.19896	-0.24364	0.02647	-0.04995	-0.03800	0.07024	0.03280	-0.10187	-0.05569	-0.15775	-0.01489	-0.12284	0.02368	0.27673	0.27167	0.07750	-0.36603	-0.43616	0.35887
HW	0.25843	-0.02751	0.15073	-0.20672	-0.04074	0.06014	-0.01078	0.05425	0.10305	-0.07771	0.02465	0.08129	-0.00720	0.10294	-0.01643	0.10419	-0.13114	0.02521	-0.24456	-0.39360
HD	0.26797	-0.10296	-0.04519	-0.12305	0.00443	0.05306	-0.00342	0.10313	0.08849	0.10223	0.21077	0.02770	-0.27135	0.23275	-0.17489	0.02733	-0.13462	-0.00542	0.05918	-0.06099
ED	0.18750	-0.17058	-0.12291	0.21677	0.20026	-0.11918	0.07169	-0.08400	-0.22772	-0.09143	0.00006	0.27884	-0.43809	0.14567	-0.37674	-0.02610	0.23732	0.13570	-0.06802	-0.12577
EE	0.21726	0.04056	-0.05532	-0.26721	-0.17648	0.03219	0.14028	0.17780	0.23664	0.20339	0.38172	-0.13237	0.20844	-0.00757	-0.17426	0.04122	0.02578	0.03310	0.03974	0.02287
ES	0.25618	-0.05870	-0.21432	-0.03512	-0.03766	-0.06978	0.04070	0.07277	-0.01510	-0.04453	-0.16704	-0.08385	-0.14497	-0.11644	-0.09137	0.02994	0.07326	0.21758	0.32941	0.13573
EN	0.04910	0.21142	-0.33265	-0.13637	-0.15298	0.01294	0.31748	0.29908	-0.06785	-0.02589	-0.21215	-0.01043	-0.08136	0.05517	0.13810	-0.01194	0.01964	-0.22604	0.20694	-0.22577
IO	0.03433	0.25460	-0.04652	0.43688	-0.06050	-0.00786	0.04767	0.09490	-0.20717	0.30963	0.25717	-0.27299	-0.05556	0.16473	-0.04355	-0.21138	0.08721	-0.08312	-0.14634	-0.25570
EL	0.23988	-0.09871	0.09134	0.09140	0.11991	0.06957	-0.23752	0.08379	0.17430	-0.00673	-0.44008	-0.20998	-0.16738	-0.14914	0.15975	-0.29579	-0.11160	-0.13625	0.02636	-0.16958
IN	0.10460	0.29067	-0.26712	-0.01227	0.02086	0.09241	-0.25190	0.05411	0.34428	-0.03287	-0.05405	0.05400	0.03651	-0.26938	-0.05641	-0.35880	0.28859	0.13277	0.06035	-0.10551
SL	0.03042	-0.08570	-0.18968	0.39462	0.18476	0.32132	-0.15084	0.24457	-0.05256	0.36923	0.02662	0.05571	0.03480	-0.33682	-0.08317	0.28187	-0.23862	0.09802	0.00251	0.13852
IL	0.06796	-0.17501	-0.17887	-0.03107	0.04336	0.58846	-0.29084	-0.27281	0.05298	-0.15828	0.23980	0.15181	-0.05294	0.13639	0.24370	0.06691	0.07551	-0.14351	0.04934	-0.02115
LRT	-0.21598	-0.20479	-0.16120	0.01813	-0.17786	0.02009	0.05508	-0.22782	-0.17821	0.04381	-0.03147	-0.17323	0.07202	-0.20551	-0.12803	-0.14512	0.13435	-0.18115	0.03118	-0.03252
VS	0.16657	0.10695	0.25741	-0.06730	-0.06220	0.37858	0.01275	0.20335	-0.27539	-0.20695	0.17918	-0.31614	-0.06740	-0.08923	0.01628	0.05376	0.31463	-0.00064	0.11030	0.04588
VSM	0.19497	0.22250	0.19478	0.00007	0.10141	0.07571	0.13400	0.05298	-0.30599	-0.02000	0.07348	0.28816	0.21509	-0.34321	-0.03537	-0.09287	-0.25553	-0.12177	-0.02719	-0.17865
TL4E	0.08179	0.06963	-0.24125	0.07221	-0.25669	-0.24095	-0.49003	0.17841	-0.25643	-0.43038	0.12722	-0.10901	0.13799	0.04737	-0.12904	0.07458	-0.05136	0.08650	-0.04076	0.04716
TL4U	-0.09077	-0.19914	0.11680	0.30482	0.06501	0.13841	0.32383	0.42890	0.23577	-0.28206	-0.04278	0.08929	0.16677	0.11200	0.15924	0.03000	0.30712	0.23677	-0.12228	0.02930
TL4T	0.14635	-0.28852	-0.03036	0.25616	-0.01746	-0.23056	-0.11246	0.17681	0.01152	-0.11924	-0.01195	0.06645	0.36676	0.11348	0.06770	0.13473	-0.15017	-0.18436	0.29905	-0.14069
FL4E	-0.15741	0.35000	-0.05401	-0.03423	-0.06923	0.12302	0.00618	0.09899	0.02003	-0.13411	0.05010	0.39827	-0.01407	0.09428	-0.14460	-0.16808	-0.19695	0.06690	0.17921	0.31557
FL4U	0.12583	-0.00056	0.21692	0.15213	-0.48415	-0.05093	-0.11422	-0.11500	0.11325	0.19106	-0.04469	-0.13621	-0.08395	0.00467	0.11694	0.02024	-0.05731	0.35380	-0.10534	0.18620
FL4T	0.18679	-0.06389	0.16536	0.14256	-0.32756	-0.11735	-0.15208	0.03423	0.09500	0.27592	0.05398	0.47501	0.04033	0.07183	0.09721	-0.14423	0.32361	-0.33680	0.06483	0.06819
FS	-0.24545	-0.12424	-0.19352	0.07820	-0.11378	0.03121	0.16632	0.04390	0.03917	0.07810	0.09106	-0.00774	-0.08024	-0.06851	-0.04951	-0.06464	0.09146	-0.12485	0.15080	0.12074
PCS	-0.11556	-0.13425	-0.33245	-0.12928	-0.31253	0.09434	0.03937	0.15262	-0.00469	0.09077	-0.08296	0.19843	-0.08665	-0.06182	0.10446	0.02770	-0.16779	0.27163	-0.33733	-0.24233
PPS	0.17026	-0.17969	0.24799	-0.23461	-0.04178	-0.00352	-0.01819	0.22251	-0.27842	0.09893	-0.16897	0.12562	-0.11035	-0.18408	-0.04763	-0.07179	0.07847	0.05889	-0.00093	0.28740
BB	-0.09732	0.32188	0.17755	0.11828	-0.17879	0.15996	-0.07129	-0.07774	0.17550	0.02930	-0.35203	0.02008	-0.05615	0.08235	-0.35779	0.53962	0.10318	-0.09477	0.16905	-0.17180

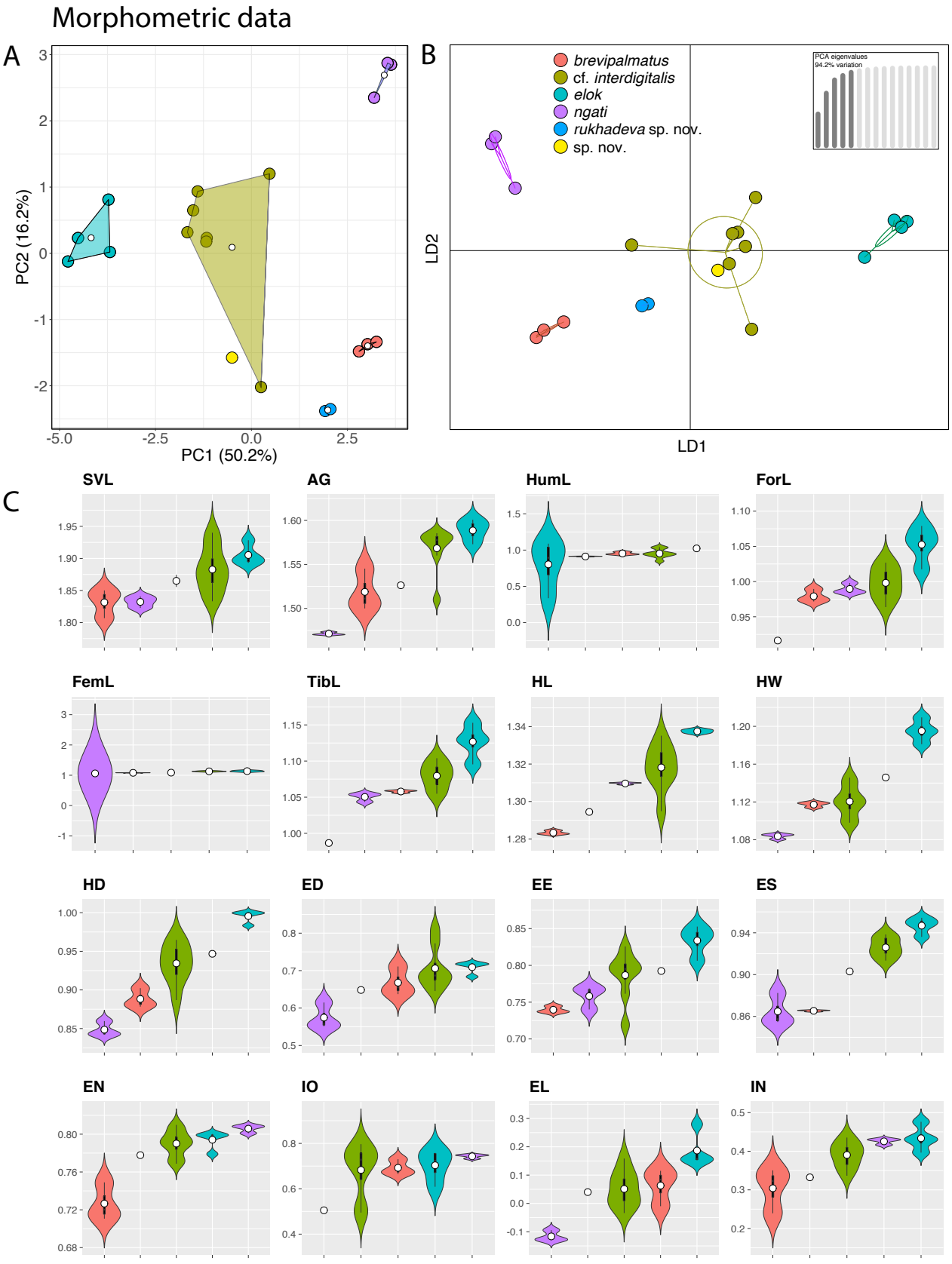

Figure 3. A. PCA of the *Cyrtodactylus brevipalmatus* group based on the adjusted morphometric data. B. DAPC of same. C. Violin plots overlain with box plots showing the range, frequency, mean (white dot), and 50% quartile (black rectangle) for each character.

midpoint of eye, second supralabial same size as first; 10(R,L) infralabials tapering smoothly to just below and slightly past posterior margin of eye; scales of rostrum and lores flat to domed, larger than granular scales on top of head and occiput; scales of occiput and interorbital region intermixed with distinct, small tubercles; superciliaries subrectngular, largest anteriorly; mental triangular, bordered laterally by first infralabials and posteriorly by

A

PCA summary statistics of morphometric characters

	PC1	PC2	PC3	PC4	PC5	PC6	PC7	PC8	PC9	PC10	PC11	PC12	PC13	PC14	PC15	PC16
Standard deviation	2.83357	1.60867	1.27741	1.01343	0.93078	0.67995	0.64342	0.58859	0.49791	0.37795	0.36543	0.24395	0.19839	0.10656	0.02424	0.00000
Proportion of variance	0.50182	0.16174	0.10199	0.06419	0.05415	0.02890	0.02587	0.02165	0.01549	0.00893	0.00835	0.00372	0.00246	0.00071	0.00004	0.00000
Cumulative proportion	0.50182	0.66356	0.76554	0.82974	0.88388	0.91278	0.93865	0.96031	0.97580	0.98473	0.99307	0.99679	0.99925	0.99996	1.00000	1.00000
Eigenvalue	8.02914	2.58781	1.63177	1.02705	0.86636	0.46233	0.41399	0.34644	0.24791	0.14285	0.13354	0.05951	0.03936	0.01136	0.00059	0.00000
SVL	-0.26747	-0.05748	0.14728	0.08652	0.18598	-0.34997	-0.70736	0.47021	0.10725	-0.01738	0.07380	0.00922	-0.00763	-0.00542	0.00614	0.00000
AG	-0.30464	-0.21303	-0.07540	0.11882	0.08863	-0.05097	0.16960	-0.09978	0.34287	-0.61461	-0.02183	-0.18853	0.34886	0.12961	-0.17538	-0.30373
HumL	0.08823	-0.21753	-0.22313	0.77711	-0.17544	-0.36367	0.03743	-0.19987	-0.05476	0.21574	0.17146	-0.01097	0.01791	-0.01657	-0.05716	0.06249
ForL	-0.25107	0.25857	-0.33924	0.01759	-0.23373	0.20343	-0.15097	0.09112	-0.32899	-0.01065	0.04980	-0.66534	-0.08806	0.10128	-0.22425	0.07613
FemL	-0.29975	-0.12436	-0.00514	0.22602	0.15496	0.42439	-0.19513	-0.21100	0.12384	0.33210	-0.46902	-0.07115	0.03682	-0.36119	0.13909	-0.23457
TibL	-0.27240	0.14949	-0.33595	0.01307	-0.20575	0.20151	-0.28988	-0.32988	0.14307	-0.30240	0.21319	0.38388	-0.16265	0.04047	0.33118	0.26856
HL	-0.29050	0.30819	0.05954	0.06005	0.08021	-0.02071	0.02826	-0.04837	-0.35874	0.12435	-0.12151	0.34101	0.65656	0.13689	-0.19043	0.20543
HW	-0.26901	-0.24493	0.11274	-0.12088	-0.46008	0.05664	-0.00036	0.06258	-0.33354	0.09172	0.24677	0.27883	-0.07324	0.01399	-0.05915	-0.59512
HD	-0.31238	-0.21054	0.10673	-0.06239	-0.05244	-0.00373	0.30534	0.20693	0.04072	0.19367	0.27984	-0.26926	0.25814	-0.01691	0.62978	0.22465
ED	-0.23239	-0.14994	-0.32012	-0.08700	0.56471	0.11441	0.19830	0.06699	-0.04452	0.14108	0.44679	0.14434	-0.16694	-0.24447	-0.32409	0.05162
EE	-0.26459	-0.03996	0.36487	0.12936	-0.37731	0.18081	0.18703	0.19955	0.34819	0.03234	-0.04299	0.09495	-0.18412	-0.11908	-0.42602	0.40737
ES	-0.33133	-0.03905	0.09431	0.06755	0.24467	-0.09713	0.16480	-0.10456	-0.04145	0.15011	-0.23722	0.03770	-0.43012	0.70470	0.06467	-0.01076
EN	-0.13074	0.39481	0.38642	0.33844	0.18379	-0.04897	0.19217	0.01203	-0.33005	-0.38059	0.06017	-0.02425	-0.26872	-0.33725	0.19053	-0.09841
IO	-0.05317	0.43050	-0.44665	0.09209	-0.11664	-0.12085	0.28188	0.48917	0.28315	0.11284	-0.19442	0.19603	-0.03729	-0.04087	0.12043	-0.26496
EL	-0.25117	-0.22022	-0.20109	-0.32394	-0.12222	-0.53668	0.10895	-0.13282	-0.20466	-0.10595	-0.41425	0.00157	-0.13675	-0.35734	-0.01246	0.19825
IN	-0.17218	0.42978	0.18290	-0.20977	-0.03884	-0.34157	-0.02879	-0.45384	0.35547	0.31606	0.26839	-0.17979	0.01476	-0.08755	-0.09257	-0.19013

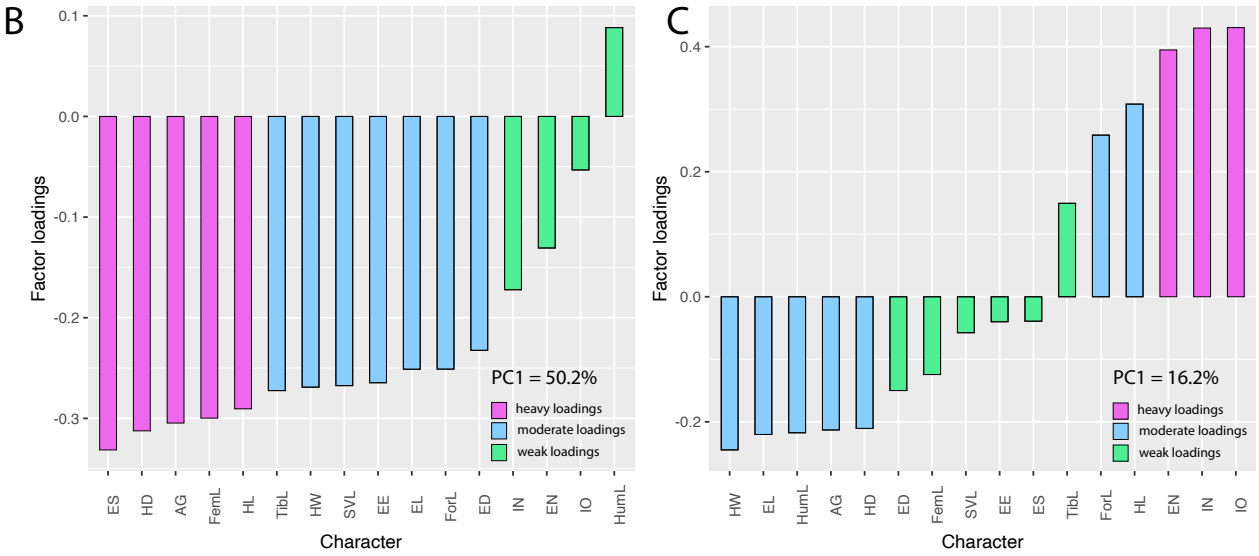

Figure 4. A. PCA summary statistics of the adjusted morphometric data of the *Cyrtodactylus brevipalmatus* group B. Factor loadings of PC1. C. Factor loadings of PC2.

large left and right trapezoidal postmentals contacting medially for 60% of their length posterior to mental; one row of slightly enlarged, elongate sublabials extending posteriorly to fifth infralabial; gular and throat scales small, granular, grading posteriorly into slightly larger, flatter, smooth, imbricate, pectoral and ventral scales.

Body relatively short (AG/SVL 0.46) with defined ventrolateral folds; dorsal scales small, granular interspersed with larger, conical, semi-regularly arranged, moderately keeled tubercles; tubercles extend from interorbital region onto base of tail; smaller tubercles extend anteriorly onto nape and occiput, diminishing in size and distinction in interorbital region; approximately 19 longitudinal rows of tubercles at midbody; approximately 27 paravertebral tubercles; 34 longitudinal rows of flat, imbricate, ventral scales much larger than dorsal scales; 153 transverse rows of ventral scales; 17 large, pore-bearing, precloacal scales; no deep precloacal groove or depression; and nine rows of post-precloacal scales on midline.

Forelimbs moderate in stature, relatively short (ForL/SVL 0.11); granular scales of forearm slightly larger than those on body, interspersed with small tubercles; palmar scales rounded, slightly raised; digits well-developed, relatively short, inflected at basal interphalangeal joints; digits narrower distal to inflections; subdigital lamellae wide, transversely expanded proximal to joint inflections, narrower transverse lamellae distal to joint inflections; claws well-developed, claw base sheathed by a dorsal and ventral scale; nine expanded and 11 unexpanded lamellae beneath first finger; hind limbs more robust than forelimbs, moderate in length (TibL/SVL 0.13), covered dorsally by granular scales interspersed with moderately sized, conical tubercles and anteriorly by flat, slightly larger scales; ventral scales of thigh flat, subimbricate, larger than dorsals; subtibial scales flat, imbricate; one row of 9,8(R,L) enlarged femoral scales not continuous with enlarged precloacal scales, terminating distally at knee; proximal femoral scales smaller than distal femorals, the latter forming an abrupt union with smaller, rounded, ventral scales of posteroventral margin of thigh; 8,9(R,L) femoral pores; plantar scales flat; digits relatively long, well-developed, inflected at basal interphalangeal joints; 8(R,L) wide, transversely expanded subdigital lamellae on fourth toe proximal to joint inflection that extend onto sole; nine expanded and 10 unexpanded lamellae beneath first toe; and claws well-developed, sheathed by a dorsal and ventral scale at base.

Tail long (TL/SVL 1.29) 6.8 mm in width at base, tapering to a point; dorsal scales flat, square bearing tubercles forming paravertebral rows and slightly larger tubercles forming a dorsolateral longitudinal row; enlarged, posteriorly directed semi-spinose tubercles forming small

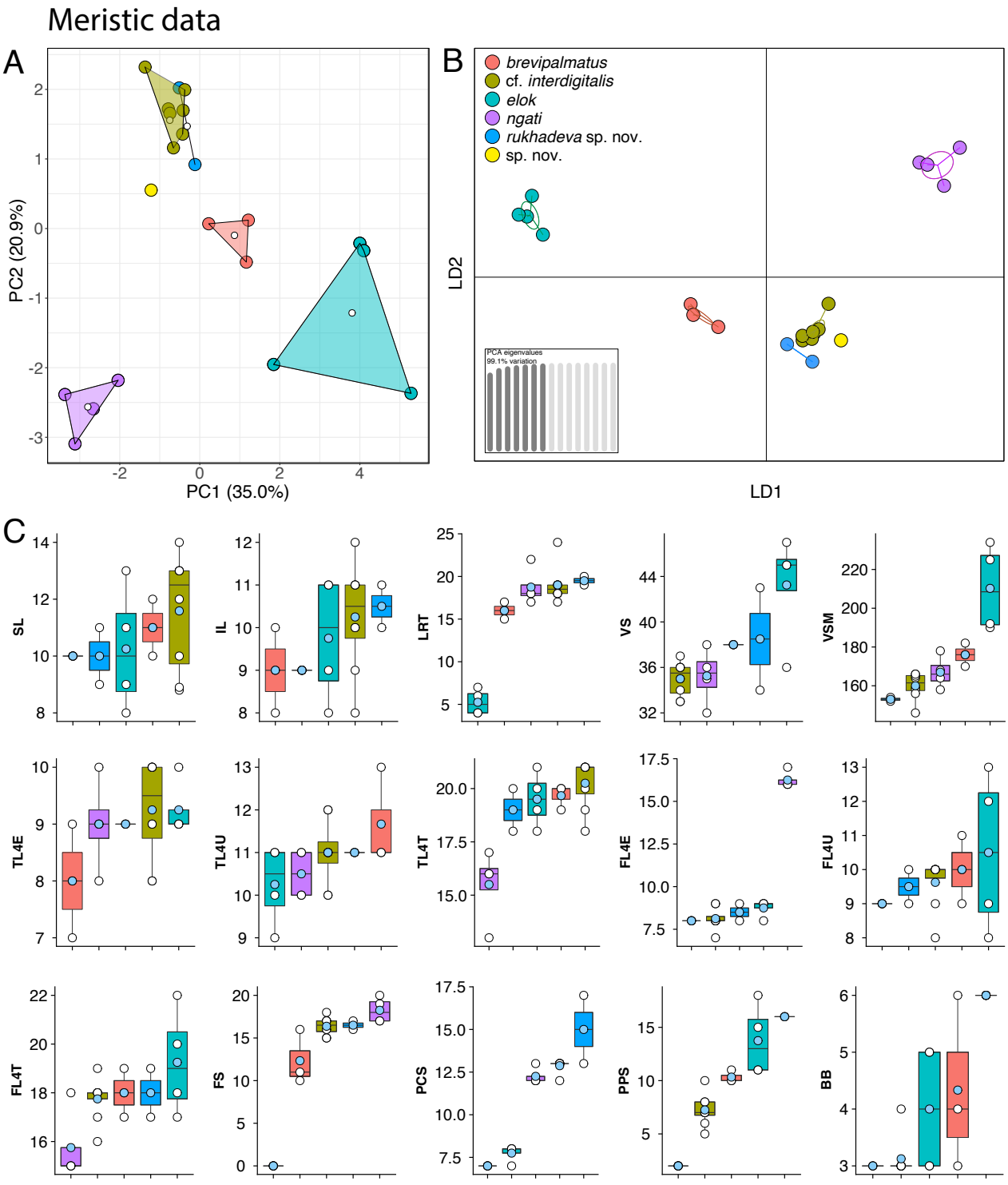

Figure 5. A. PCA of the *Cyrtodactylus brevipalmatus* group based on the meristic data. B. DAPC of same. C. Box plots showing the range, frequency, mean (blue dot), and 50% quartile (black rectangle) for each character. White dots are values on y-axis.

but distinct ventrolateral caudal fringe; median row of paired, transversely expanded subcaudal scales, larger than dorsal caudal scales; base of tail bearing hemipenal swellings; three conical postcloacal tubercles at base of hemipenal swellings; and postcloacal scales flat, imbricate.

Coloration in life (Fig. 8). Ground color of the head body, limbs, and tail brown; faint, diffuse mottling on the top of the head; wide, dark-brown post-orbital stripe; lores dark- brown; nuchal band faint, bearing two posterior projections; three wide faint body bands edged in dark-brown between limb insertions; band interspaces bearing irregularly shaped, dark markings; faint dark speckling on limbs and digits; five wide slightly darker caudal bands separated by five lighter caudal bands; posterior tip of regenerated tail unbanded; ventral surfaces beige, generally immaculate; gular region lacking pigment; poaterior subcaudal region faintly banded; iris orangish gold in color.

PCA summary statistics of meristic characters

A

Meristic data	PC1	PC2	PC3	PC4	PC5	PC6	PC7	PC8	PC9	PC10	PC11	PC12	PC13	PC14	PC15
Standard deviation	2.29166	1.77351	1.25761	1.17184	1.11116	0.94747	0.71022	0.59682	0.49770	0.39953	0.35572	0.26720	0.18042	0.11315	0.06739
Proportion of variance	0.35011	0.20969	0.10544	0.09155	0.08231	0.05985	0.03363	0.02375	0.01651	0.01064	0.00844	0.00476	0.00217	0.00085	0.00030
Cumulative proportion	0.35011	0.55980	0.66524	0.75679	0.83910	0.89895	0.93258	0.95632	0.97284	0.98348	0.99191	0.99667	0.99884	0.99970	1.00000
Eigenvalue	5.25172	3.14534	1.58158	1.37322	1.23467	0.89771	0.50442	0.35619	0.24771	0.15962	0.12654	0.07140	0.03255	0.01280	0.00454
SL	-0.01465	0.28619	-0.10727	-0.26780	-0.64507	-0.03924	0.09355	-0.37301	0.44147	-0.18831	0.00356	-0.10645	-0.14364	0.02476	0.07853
IL	0.02171	0.28741	0.08318	-0.48619	-0.05064	-0.59507	0.21144	0.22548	-0.37802	0.08215	-0.16176	0.06952	-0.06264	0.04421	-0.18676
LRT	-0.35828	0.17923	0.05539	0.20214	0.13945	-0.18144	0.10880	0.12761	0.40480	0.47558	-0.40331	0.05971	-0.07083	0.13653	0.36767
VS	0.34214	-0.12468	-0.08963	-0.08773	-0.04034	-0.40906	-0.42066	0.31099	0.30806	0.09514	0.21478	-0.20900	0.22517	-0.31629	0.25402
VSM	0.34223	-0.24318	-0.08109	-0.17610	-0.11866	0.05748	-0.17573	-0.32681	0.05406	0.61389	-0.10077	0.34783	0.10667	0.18893	-0.27035
TL4E	0.03335	0.08813	0.66639	-0.13592	-0.19725	0.29074	-0.36243	0.35739	0.09978	-0.01419	-0.10741	-0.12631	-0.03963	0.29506	-0.14064
TL4U	-0.03361	0.24541	-0.49197	0.34300	-0.31988	-0.03117	-0.41635	0.24476	-0.29234	-0.00856	-0.00174	0.11443	-0.13485	0.35288	0.03276
TL4T	0.20535	0.43914	0.04338	0.11313	-0.15440	0.31816	0.02412	0.12482	-0.10359	0.07859	-0.26520	0.30953	0.15211	-0.63448	0.01854
FL4E	-0.23859	-0.40764	0.11346	-0.04385	-0.21966	-0.06278	-0.28136	-0.16144	-0.30134	0.09616	-0.24925	-0.10943	-0.50633	-0.38466	0.16190
FL4U	0.25822	0.00381	0.31427	0.50023	-0.12421	-0.29169	0.21540	0.04112	0.13469	0.04876	0.34106	0.24152	-0.44886	-0.05669	-0.18934
FL4T	0.33291	0.14301	0.22877	0.31958	-0.11392	-0.10392	0.10909	-0.34341	-0.35094	0.14907	-0.12988	-0.50485	0.24573	0.14157	0.25119
FS	-0.39492	0.14962	-0.05372	0.20445	-0.03815	-0.10710	-0.13810	-0.07734	0.08946	0.22271	0.06379	-0.38499	0.17407	-0.23560	-0.66580
PCS	-0.28428	0.22523	0.31077	0.02848	0.13565	-0.25746	-0.42079	-0.42839	-0.08212	-0.16560	0.20366	0.40866	0.24329	-0.00220	0.15476
PPS	0.33736	0.12717	-0.08939	0.07725	0.39769	-0.14568	-0.26179	-0.19406	0.21036	-0.35223	-0.52488	-0.06710	-0.25247	0.02805	-0.24008
BB	-0.08569	-0.43809	0.06695	0.24607	-0.35558	-0.23509	0.13945	0.11897	0.05719	-0.32299	-0.39578	0.21411	0.44044	0.03742	-0.12219

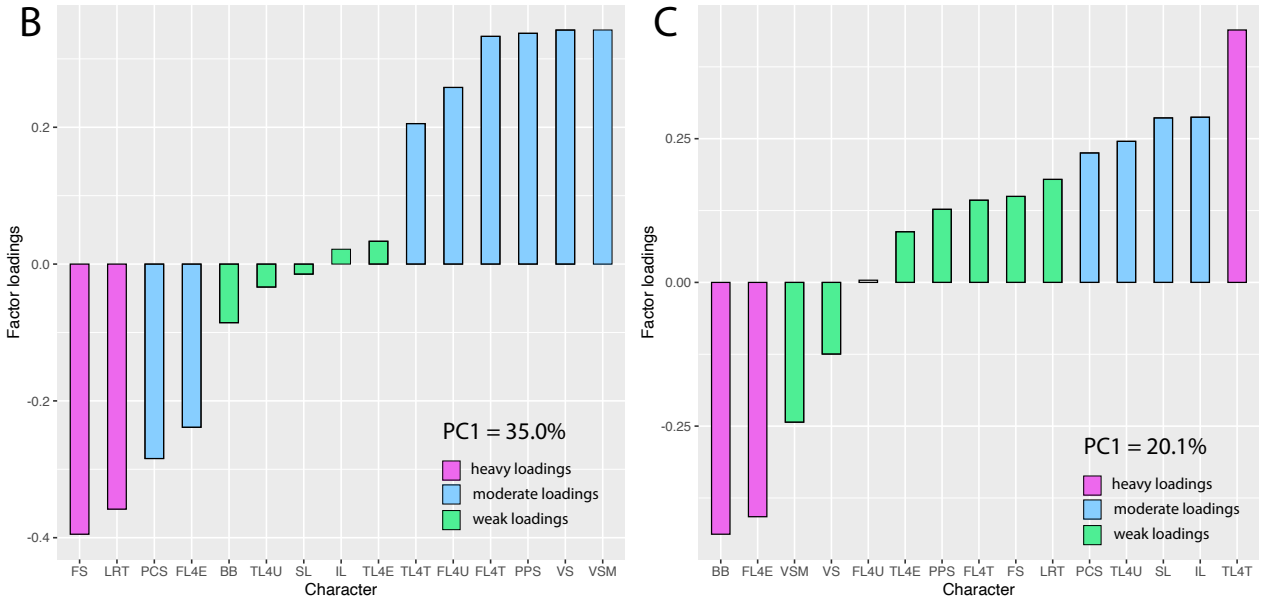

Figure 6. A. PCA summary statistics of the meristic data of the *Cyrtodactylus brevipalmatus* group B. Factor loadings of PC1. C. Factor loadings of PC2.

Variation (Fig. 8). The female paratype differs significantly from the male holotype in coloration and pattern. The holotype has a much less contrasting dorsal pattern with only faint indications of dorsal body and caudal bands whereas the paratype is boldly marked, bearing a one dark jagged-edged nuchal band and three dark jagged-edged body bands, all with darkened borders. The caudal pattern of the paratype consists of six dark and seven light-colored contrasting bands on a full original tail whereas the holotype has four dark and light-colored weakly contrasting bands and a regenerated tail tip. The top of the head of the holotype is essentially unicolor whereas that of the paratype is darkly mottled. With only one specimen of each sex we cannot say if these differences in color pattern are sexually dimorphic. An uncataloged juvenile had a generally unicolor tan dorsal ground color overlain with a dark-brown nuchal loop bearing two posteriorly oriented projections, four complete to incomplete dark-brown body bands, and nine dark-brown caudal bands separated by eight tan to white caudal bands (Fig. 8)

Distribution. *Cyrtodactylus rukhadeva* sp. nov. is known only from the type locality from Khao Laem Mountain, Suan Phueng District, Ratchaburi Province, Thailand and Hoop Phai, Suan Phueng District, Ratchaburi Province, approximately 7.7 km to the west of the type locality (Fig. 1).

Etymology. The specific epithet "*rukhadeva*" is given as a noun in apposition and refers to the spirits or gods residing in trees in Thai mythology, known as Rukha Deva (literally "Tree Nymphs"). According to Thai folklore, these sylvan spirits live on tree branches and on large older trees wearing traditional Thai attire, usually in reddish or brownish colours, and are believed to protect the forest. The new arboreal species of *Cyrtodactylus* resides in one of the remaining fragments of the north Tenasserim montane forests. We want to underscore the need for the immediate assessment of herpetofaunal diversity surveys and implementation of adequate conservation measures for these relic forests.

Comparisons. Given the low sample size (n=2) of *Cyrtodactylus rukhadeva* sp. nov., meaningful statistical comparisons of meristic were not possible. However, some character ranges—at this point—are diagnostic in that they are widely separated from one another. We are

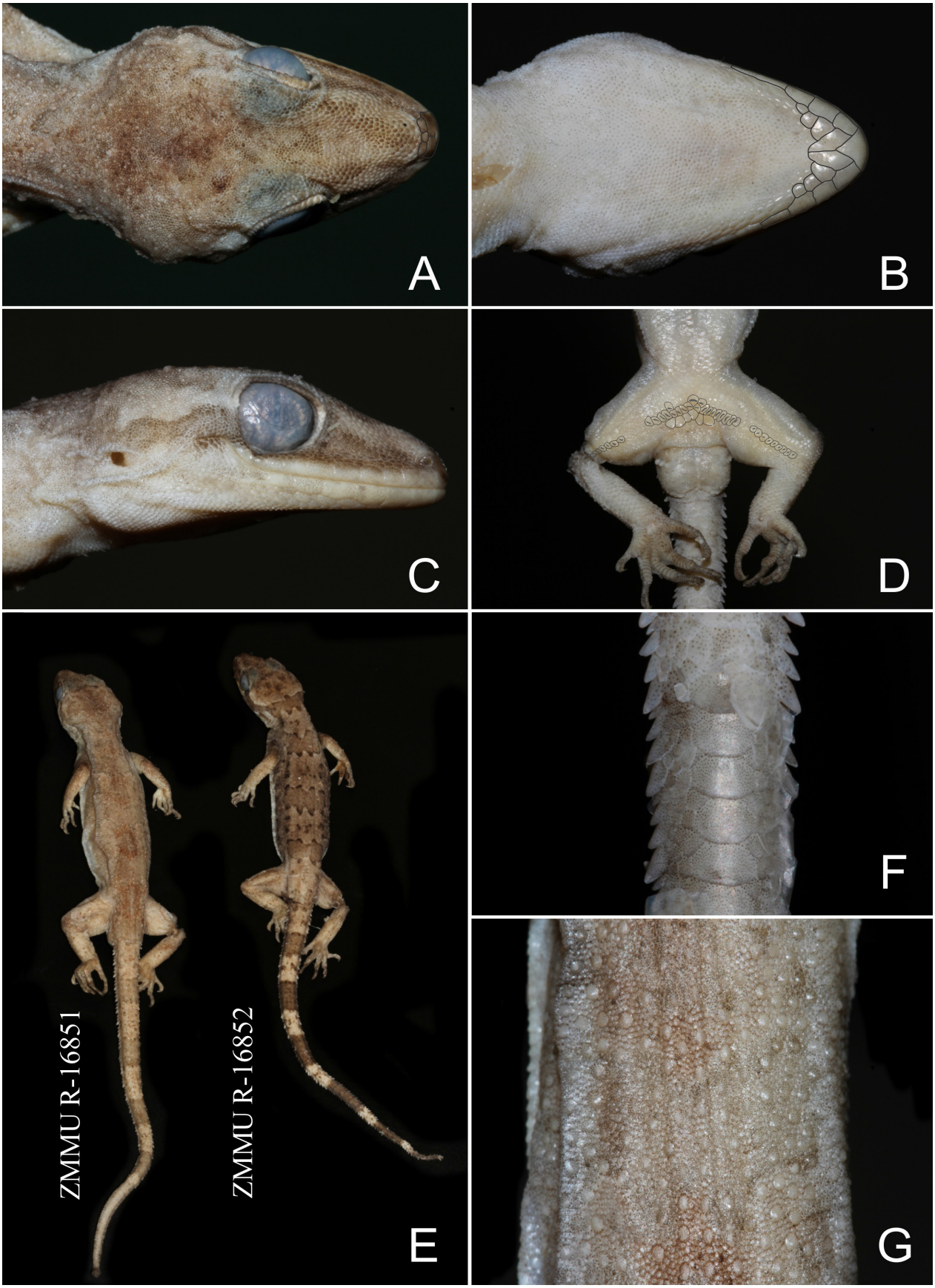

Figure 7. A. Dorsal view of the head of the holotype of *Cyrtodactylus rukhadeva* **sp. nov.** (ZMMU R-16851) from Khao Laem Mountain, Suan Phueng District, Ratchaburi Province, Thailand. B. Gular region of the holotype. C. Right lateral view of the head of the holotype. D. Pores in the femoral and precloacal region of the holotype. E. Dorsal views of the holotype (left) and paratype (ZMMU R-16852) from Hoop Phai Tong, Suan Phueng District, Ratchaburi Province, Thailand. F. Subcaudal region of the holotype showing the single median row of transversely enlarged subcaudal scales. G. Dorsal view of body showing the tubercles intermixed with granular scales. Photos by Roman A. Nazarov.

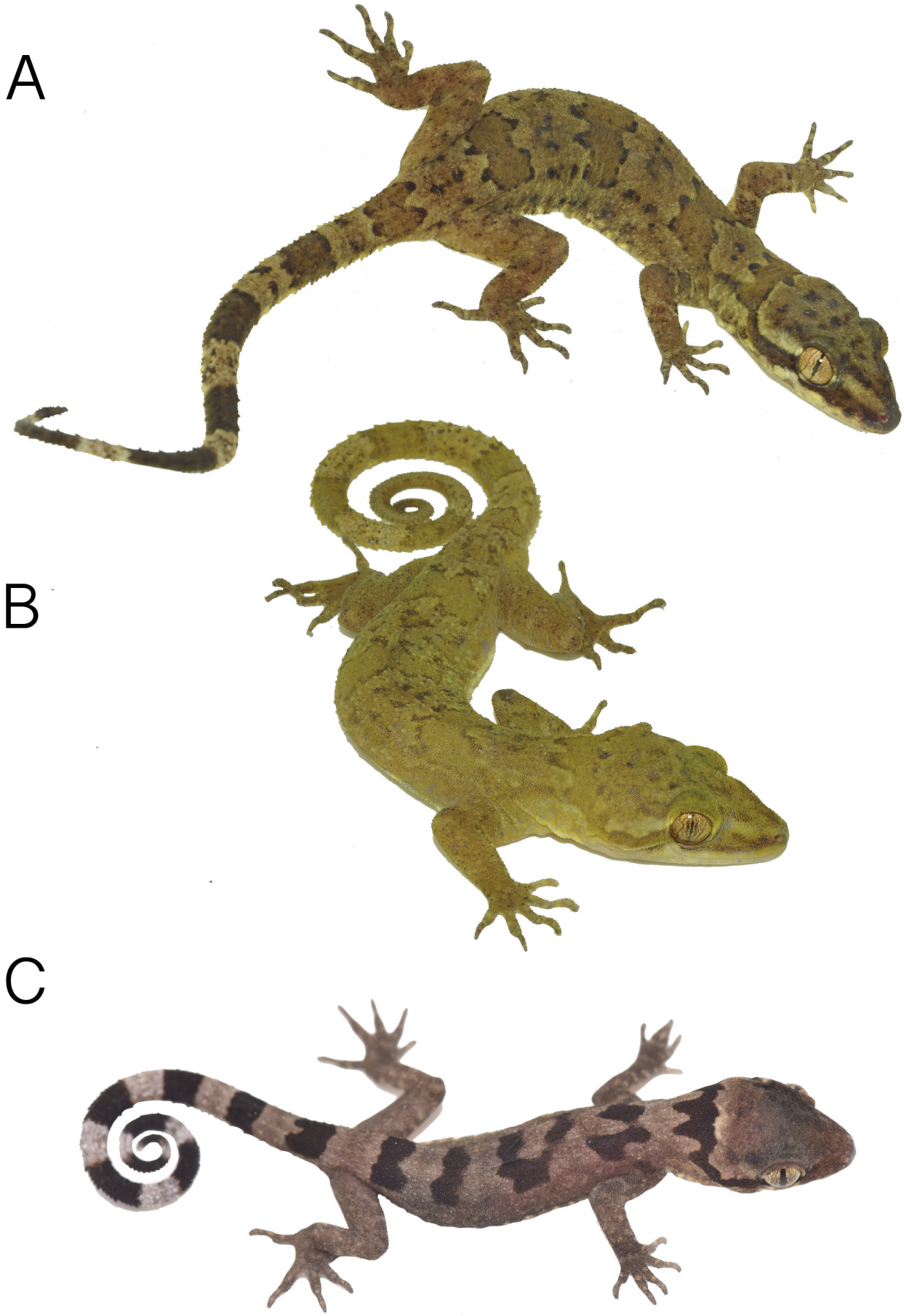

Figure 8. In life coloration and pattern of (A) the paratype of *Cyrtodactylus rukhadeva* sp. nov. (ZMMU R-16852) from Hoop Phai Trong, Suan Phueng District, Ratchaburi Province, Thailand and (B) the holotype (ZMMU R-16581) from Khao Laem Mountain, Suan Phueng District, Ratchaburi Province, Thailand. Photos by Platon V. Yushchenko. C. In life coloration and pattern of a hatchling of *Cyrtodactylus rukhadeva* **sp. nov.** (not collected); photo by Mali Naiduangchan.

Table 4. Distribution of discrete character data among the species of the *Cyrtodactylus brevipalmatus* group. Shaded cells denote diagnostic character differences from *C. rukhadeva* sp. nov. / = data unavailable.

	***rukhadeva* sp. nov.**	***rukhadeva* sp. nov.**	**sp. nov.**	**cf. *interdigitalis***	**cf. *interdigitalis***	**cf. *interdigitalis***	**cf. *interdigitalis***	**cf. *interdigitalis***	**cf. *interdigitalis***	**cf. *interdigitalis***	
	Holotype, ZMMU R-16851	Paratype ZMMU R-16852	ZMMU R-16492 (field tag NAP 08236)	ZMMU R-14917	NCSM 79472	NCSM 80100	FMNH 255454	FMNH 265806	FMNH 270492	FMNH 270493	
iris	yellow-gold	yellow-gold	yellow-gold	yellow-gold	/	/	/	/	yellow-gold		
/paravertebral tubercles	present	present	present	present	present	present	present	present	present	present	
enlarged femoral scales	present	present	present	present	present	present	present	present	present	present	
small tubercles on forelimbs	present	present	present	absent	absent	absent	absent	absent	present	present	
small tubercles on flank	present	present	present	present	present	present	present	present	present	present	
femoral pores	present	present	present	present	present	present	present	present	present	present	
dorsolateral caudal tubercles	small	small	small	small	small	small	small	small	small	small	
ventrolateral caudal fringe	small	small	small	small	small	small	small	small	small	small	
tail crossection	square	square	round	round	round	round	round	round	round	round	
enlarged subcaudals	present	present	present	present	present	present	present	present	present	present	
paired enlarged subcaudal scales	absent	absent	present	present	present	present	present	present	present	present	
single enlarged subcaudal scales	present	present	absent	absent	absent	absent	absent	absent	absent	absent	
prehensile tail	present	present	present	present	present	present	present	present	present	present	
	ngati	***ngati***	***ngati***	***ngati***	***elok***	***elok***	***elok***	***elok***	***brevipalmatus***	***brevipalmatus***	***brevipalmatus***
	HNUE-R00111 holotype	IEBR 4829 (Paratype)	VNUF R.2020.12 (Paratype)	HNUE-R00112 (Paratype)	LSUHC 8238	LSUHC 12180	LSUHC 12181	ZMMU R-16144	LSUHC 1899	LSUHC 15076	LSUHC 11787
iris	yellow-gold	/	yellow-gold	/	silver-white	silver-white	silver-white	/	silver-white	silver-white	silver-white
paravertebral tubercles	present	present	present	present	absent	absent	absent	absent	present	present	present
enlarged femoral scales	present	present	present	present	absent	absent	absent	absent	present	present	present
small tubercles on forelimbs	absent	absent	absent	absent	absent	absent	absent	absent	present	present	present
small tubercles on flank	present	present	present	present	absent	absent	absent	absent	present	present	present
femoral pores	present	present	present	present	absent	absent	absent	absent	present	present	present
dorsolteral caudal tubercles	small	small	small	small	large	large	large	large	small	small	small
enlarged subcaudals	absent	absent	absent	absent	absent	absent	absent	absent	present	present	present

Table 4 continued.

	ngati	***ngati***	***ngati***	***ngati***	***elok***	***elok***	***elok***	***elok***	***brevipalmatus***	***brevipalmatus***	***brevipalmatus***
	HNUE-R00111 holotype	IEBR 4829 (Paratype)	VNUF R.2020.12 (Paratype)	HNUE-R00112 (Paratype)	LSUHC 8238	LSUHC 12180	LSUHC 12181	ZMMU R-16144	LSUHC 1899	LSUHC 15076	LSUHC 11787
ventrolateral caudal fringe	small	small	small	small	large	large	large	large	small	small	small
tail crossection	round	round	round	round	square	square	square	square	round	round	round
paired enlarged subcaudal scales	absent	absent	absent	absent	absent	absent	absent	absent	present	present	present
single enlarged subcaudal scales	absent	absent	absent	absent	absent	absent	absent	absent	absent	absent	absent
prehensile tail	absent	absent	absent	absent	present	present	present	present	present	present	present

well aware that a larger sample size may preclude some of these characters as being diagnostic but it is equally probable that they will demonstrate that they are truly diagnostic. *Cyrtodactylus rukhadeva* sp. nov. can be separated from *C. ngati* in having fewer paravertebral tubercles (PVT; 27–30 vs 38–40), from *C. elok* in having more longitudinal rows of dorsal tubercles (LRT; 19 or 20 vs 4–7), from *C. brevipalmatus* and *C. elok* in having fewer transverse rows of ventral scales (VSM; 152–154 vs 172–180 and 190–234, respectively), from *C. brevipalmatus* in having more enlarged femoral scales (FS; 16 or 17 vs 10–16), from all species in having more femoral pores in males (FP; 20 vs 0–17 collectively), from *C.* cf. *interdigitalis, C. brevipalmatus,* and *C. elok* in having males having more precloacal pores (PP; 17 vs 13, 7, and 8, respectively), and from all species except *C. elok* in having more post-precloacal scales (PPS; 16 vs 2–10, cllectively. All ranges are presented in Table 5. Summary statistics and comparisons among the adjusted morphometric characters are presented in Table 6.

Cyrtodactylus rukhadeva sp. nov. can be readily separated from all other species on the basis of discrete morphological differences (Table 4). *Cyrtodactylus rukhadeva* sp. nov. has paravertebral tubercles and enlarged femoral scales which are absent in *C. elok. Cyrtodactylus rukhadeva* sp. nov. has small tubercles on the forelimbs which are absent in *C.* cf. *interdigitalis, C. ngati,* and *C. elok. Cyrtodactylus rukhadeva* sp. nov. has small tubercles on the flanks, femoral pores in males, enlarged dorsolateral tubercles, and a large ventrolateral caudal fringe that are absent in *C. elok. Cyrtodactylus rukhadeva* sp. nov. has a square tail in cross-section versus a round tail in *C.* cf. *interdigitalis, C. ngati,* and *C. brevipalmatus. Cyrtodactylus rukhadeva* sp. nov. has single enlarged subcaudal scales versus paired enlarged subcaudal scales in *C.* cf. *interdigitalis* and *C. brevipalmatus. Cyrtodactylus elok* and *C. ngati* lack distinctly enlarged subcaudal scales. *Cyrtodactylus rukhadeva* sp. nov. has a prehensile tail apparently lacking in *C. ngati*. Figure 9 illustrates the general morphological and color pattern similarity of the other members of the *brevipalmatus* group to *C. rukhadeva* sp. nov.

Natural History. *Cyrtodactylus rukhadeva* sp. nov. inhabits montane and submontane evergreen polydominant tropical forests, and was most often recorded in bamboo forests mixed with dry dipterocarp forests at elevations ranging from 600 to 1100 m a.s.l. and dominated by the large trees *Anisoptera costata* Korth, 1841 and *Dipterocarpus gracilis* Blume, 1825 (Dipterocarpaceae) (Fig. 10A). Lizards were usually observed near large tree holes or hiding among the roots of strangler fig trees (*Ficus* sp.; Moraceae) (Fig. 10B). All were active from approximately 19:30–23:50 hrs and approximately 2 m above the ground. One lizard was observed ca. 6 m above the ground on the branch of *Syzygium* sp. (Myrtaceae) above a rocky streambed. Given its morphology, we believe *C. rukhadeva* sp. nov. is an arboreal specialist that generally resides in the upper canopy, but may be forced down to lower portions of the canopy or to the

Table 5. Summary statistics of meristic characters. sd = standard deviation and n= sample size. * = males only. Shaded cells denote diagnostic character differences from *C. rukhadeva* sp. nov. Abbreviations are in the Materials and methods.

***rukhedeva* sp. nov.**	**SL**	**IL**	**PVT**	**LRT**	**VS**	**VSM**	**TL4E**	**TL4U**	**TL4T**	**FL4E**	**FL4U**	**FL4T**	**FS**	**FP***	**PP***	**PCS**	**PPS**	**BB**
mean	10	10.5	28.5	19.5	38.5	153	9	11	19	8.5	9.5	18	16.5	20	17	15	16	3
±1 sd	1.41	0.71	1.41	0.71	6.36	1.41	0	00.00	1.41	0.71	0.71	1.41	0.71	0.00	0.00	2.83	0	0
minimum	9	10	27	19	34	152	9	11	18	8	9	17	16	20	17	13	16	3
maximum	11	11	30	20	43	154	9	11	20	9	10	19	17	20	17	17	16	3
n	2	2	2	2	2	2	2	2	2	2	2	2	2	1	1	2	2	2
ngati																		
mean	10	9	39.5	18.8	35.3	167.0	9.0	10.3	19.25	7.25	8.5	15.8	18.3	14	0	12.3	2	6
±1 sd	0	0	1.32	2.22	2.50	8.41	0.82	0.58	1.73	0.50	0	1.5	1.5	0.00	0	0.5	0	0
minimum	10	9	38	17	32	158	8	9	18	7	8	15	17	14	0	12	2	6
maximum	10	9	40	22	38	178	10	11	20	8	9	18	20	14	0	13	2	6
n	4	4	4	4	4	4	4	4	4	4	4	4	4	1	1	4	4	4
cf. *interdigitalis*																		
mean	12	10.1	28.1	19.1	35.1	162.0	9.3	10.9	20.1	8.1	9.6	17.7	16.3	14.0	13	13.1	7.1	3.1
±1 sd	2.05	1.28	1.77	2.14	1.51	6.87	0.89	0.76	1.16	0.64	0.74	0.89	1.06	1.00	0.00	0.35	1.49	0.35
minimum	9	8	26	17	33	146	8	10	18	7	8	16	15	13	13	12	5	3
maximum	14	12	32	24	37	166	10	12	21	9	10	19	18	15	13	13	10	4
n	7	7	7	7	7	7	7	7	7	7	7	7	7	2	2	7	7	7
brevipalmatus																		
mean	11	9	38.0	16	38	176	8	11.7	19.7	8.0	10.0	18.0	12.3	7	7	7.0	10.3	4.3
±1 sd	1.00	1.00	1.00	1.00	0	6	1.00	1.15	0.58	0	1.00	1.00	3.21	0.00	0.00	0	0.58	1.53
minimum	10	8	37	15	38	170	7	11	19	8	9	17	10	7	7	7	10	3
maximum	12	10	39	17	38	182	9	13	20	8	11	19	16	7	7	7	11	6
n	3	3	3	3	3	3	3	3	3	3	3	3	3	1	1	3	3	3
elok																		
mean	10.3	9.8	0	5.3	43.3	210.3	9.3	10.3	19.5	8.8	10.5	19.3	0	0	8	7.8	13.8	4.0
±1 sd	2.22	1.50	0	1.50	4.92	22.54	0.50	0.96	1.29	0.50	2.38	2.22	0	0	0.00	0.50	3.40	1.15
minimum	8	8	0	4	36	190	9	9	18	8	8	17	0	0	8	7	11	3
maximum	13	11	0	7	47	234	10	11	21	9	13	22	0	0	8	8	18	5
n	4	4	4	4	4	4	4	4	4	4	4	4	4	4	1	4	4	4
sp. 11																		
mean	8	9	30	18	34	160	9	10	19	10	9	19	17	17	13	13	8	3
±1 sd	0.00	0.00	0.00	0.00	0.00	0.00	0.00	0.00	0.00	0.00	0.00	0.00	0.00	0.00	0.00	0.00	0.00	0
minimum	8	8	30	18	34	160	9	10	19	10	9	19	17	17	13	13	8	3
maximum	8	9	30	18	34	160	9	10	19	10	9	19	17	17	13	13	8	3
n	1	1	1	1	1	1	1	1	1	1	1	1	1	1	1	1	1	1

Table 6. Summary statistics of adjusted morphometric characters. sd = standard deviation and n= sample size. Abbreviations are in the Materials and methods.

***rukhadeva* sp. nov.**	**SVL**	**AG**	**HumL**	**ForeaL**	**FemurL**	**TibL**	**HL**	**HW**	**HD**	**ED**	**EE**	**ES**	**EN**	**IO**	**EL**	**IN**
mean	1.865	1.526	1.023	0.916	1.086	0.987	1.294	1.146	0.947	0.648	0.792	0.903	0.778	0.505	0.040	0.332
±1 sd	0.0134	0	0	0	0	0	0	0	0	0	0	0	0	0	0	0
minimum	1.8555	1.5263	1.0233	0.9163	1.0863	0.9866	1.2944	1.1459	0.9468	0.6483	0.7924	0.9030	0.7778	0.5051	0.0400	0.3324
maximum	1.8745	1.5263	1.0233	0.9163	1.0863	0.9866	1.2944	1.1459	0.9468	0.6483	0.7924	0.9030	0.7778	0.5051	0.0400	0.3324
n	2	2	2	2	2	2	2	2	2	2	2	2	2	2	2	2
ngati																
mean	1.832	1.471	0.912	0.990	1.061	1.050	1.310	1.084	0.849	0.575	0.758	0.865	0.806	0.743	-0.116	0.426
±1 sd	0.0090	0.0017	0.0043	0.0074	0.0000	0.0059	0.0005	0.0027	0.0096	0.0350	0.0157	0.0153	0.0042	0.0091	0.0192	0.0078
minimum	1.8228	1.4702	0.9070	0.9846	1.0607	1.0435	1.3090	1.0806	0.8422	0.5513	0.7401	0.8546	0.8010	0.7325	-0.1292	0.4166
maximum	1.8407	1.4732	0.9148	0.9980	1.0607	1.0543	1.3100	1.0855	0.8596	0.6148	0.7687	0.8824	0.8086	0.7489	-0.0943	0.4308
n	3	3	3	3	3	3	3	3	3	3	3	3	3	3	3	3
cf. *interdigitalis*																
mean	1.883	1.568	0.954	0.998	1.129	1.080	1.318	1.121	0.934	0.706	0.787	0.926	0.790	0.683	0.051	0.390
±1 sd	0.0361	0.0249	0.0617	0.0225	0.0137	0.0181	0.0123	0.0167	0.0259	0.0574	0.0329	0.0094	0.0138	0.1168	0.0636	0.0332
minimum	1.8331	1.5100	0.8481	0.9638	1.1106	1.0549	1.2949	1.0981	0.8869	0.6455	0.7191	0.9134	0.7688	0.4949	-0.0339	0.3367
maximum	1.9400	1.5854	1.0400	1.0268	1.1482	1.1039	1.3351	1.1458	0.9648	0.8125	0.8257	0.9384	0.8098	0.7966	0.1584	0.4354
n	8	8	8	8	8	8	8	8	8	8	8	8	8	8	8	8
brevipalmatus																
mean	1.831	1.519	0.953	0.979	1.080	1.058	1.283	1.117	0.888	0.668	0.740	0.865	0.727	0.692	0.063	0.304
±1 sd	0.0222	0.0235	0.0208	0.0092	0.0055	0.0017	0.0011	0.0027	0.0125	0.0384	0.0046	0.0007	0.0200	0.0338	0.0650	0.0579
minimum	1.8069	1.5000	0.9368	0.9718	1.0743	1.0559	1.2825	1.1141	0.8783	0.6372	0.7360	0.8645	0.7106	0.6653	-0.0098	0.2393
maximum	1.8500	1.5452	0.9768	0.9895	1.0848	1.0593	1.2846	1.1194	0.9023	0.7110	0.7449	0.8659	0.7490	0.7303	0.1151	0.3504
n	4	4	4	4	4	4	4	4	4	4	4	4	4	4	4	4
elok																
mean	1.905	1.589	0.803	1.053	1.136	1.127	1.337	1.195	0.996	0.709	0.834	0.947	0.794	0.703	0.187	0.434
±1 sd	0.0161	0.0121	0.3410	0.0259	0.0223	0.0237	0.0010	0.0116	0.0082	0.0171	0.0199	0.0078	0.0101	0.0699	0.0619	0.0327
minimum	1.8932	1.5730	0.3367	1.0175	1.1118	1.0955	1.3363	1.1811	0.9833	0.6836	0.8063	0.9361	0.7790	0.6088	0.1532	0.3965
maximum	1.9284	1.6007	1.0886	1.0790	1.1629	1.1529	1.3387	1.2094	1.0008	0.7201	0.8527	0.9544	0.8001	0.7583	0.2797	0.4762
n	4	4	4	4	4	4	4	4	4	4	4	4	4	4	4	4
sp. 11																
mean	1.940	1.571	1.031	0.979	1.145	1.071	1.311	1.139	0.921	0.645	0.793	0.915	0.788	0.508	0.015	0.337
±1 sd	0.0000	0.0000	0.0000	0.0000	0.0000	0.0000	0.0000	0.0000	0.0000	0.0000	0.0000	0.0000	0.0000	0.0000	0.0000	0.0000
minimum	1.940	1.571	1.031	0.979	1.145	1.071	1.311	1.139	0.921	0.645	0.793	0.915	0.788	0.508	0.015	0.337
maximum	1.940	1.571	1.031	0.979	1.145	1.071	1.311	1.139	0.921	0.645	0.793	0.915	0.788	0.508	0.015	0.337
n	1	1	1	1	1	1	1	1	1	1	1	1	1	1	1	1

Figure 9. Illustration showing the general similarity body shape and color pattern among five species of the *Cyrtodactylus brevipalmatus* group. A. Adult female *C. elok* (LSUDPC 2589) from Negeri Sembian, Peninsular Malaysia. Photo by L. Lee Grismer. B Adult male sp. 11 (ZMMU R-16492) from Phu Hin Rong Kla National Park, Petchabun Province, Phitsanulok, Thailand. Photo by Nikolay A. Poyarkov. C. Adult female *C. interdigitalis* from Tak Mal National Park, Phetchabun Province, Thailand. Photo from Creative Commons Attribution Share Alike. Photo by Evan S. H. Quah. D. Adult female *C.* cf. *interdigitalis* (NCSM 79472) from Ban Pha Liep, Houay Liep Stream, Xaignabouli Province, Laos. Photo by Bryan L. Stuart. E. Adult female *C. ngati* (VNUF R.2020.12) from Pa Thom Cave, Pa Xa Lao Village, Pa Thom Commune, Dien Bien District, Dien Bien Province, Vietnam. Photo by Dzung T. Le. F. Adult female *C. brevipalmatus* from the type locality at Khao Luang National Park, Nakon Si Thammarat Provice, Thailand. Photo from Creative Commons Attribution Share Alike. G. Adult male *C.* cf. *ruhkhadeva* sp. nov. form Kaeng_Krachan National Park, Petchaburi Province, Thailand. Photo from Creative Commons Attribution Share Alike.

understory layer by rain storms or strong winds. Gravid females bearing two eggs were recorded in March; two eggs of the new species were found attached in a tree hole; total length of the hatchlings was approximately 7 cm. *Cyrtodactylus rukhadeva* sp. nov. is a highly aggressive species that opens its mouth and waves its tail from side to side in a defensive posture when threatened. At the type locality, *C. rukhadeva* sp. nov. was recorded in sympatry with *Cnemaspis selenolagus* Grismer, Yushchenko, Pawangkhanant, Nazarov, Naiduangchan, Suwannapoom & Poyarkov, 2020, *Cyrtodactylus* cf. *oldhami* (Theobald, 1876), and *Gekko* (*Ptychozoon*) *kaengkrachanense* (Sumontha, Pauwels, Kunya, Limlikhitaksorn, Ruksue, Taokratok, Ansermet & Chanhome, 2012).

Figure 10. Habitat of *Cyrtodactylus rukhadeva* sp. nov. at the type locality: Khao Laem Mountain, Suan Phueng District, Ratchaburi Province, Thailand. (A) Submontane forest on the slopes of Khao Laem Mountain. (B) A male of the new species hiding among the roots of a strangler fig (*Ficus* sp.). Photos by Parinya Pawangkhanant.

Discussion

The tangled taxonomic history among the species of the *brevipalmatus* group revolves around their general morphological similarity (Fig. 9)—likely resulting from selection pressures from their unique, secretive, arboreal life style—and the fact that no detailed morphological analysis incorporating genetic data had ever been conducted. Smith's (1935) report of *C. brevipalmatus* from Ban Pa Che, Raheang (Umphang in Ellis and Pauwels 2012) Tak Province in western Thailand (not listed by Taylor 1963) was based on material he did not examine and his account merely re-described his specimens from the type locality at Khao Luang, Nakon Sri Thammarat Province (Smith 1923, 1930). Ban Pa Che is the same locality as Chao Doi Waterfall, Mae Moei National Park, Tha Song Yang District from where Chomdej et al. (2021) report sp.10. and it is highly likely this is the species reported by Smith (1935) as *C. brevipalmatus*. Ulber (1993) examined a specimen he referred to as *C. brevipalmatus* from Kaeng Krachen National Park, Petchaburi Province, approximately 400 km north of the type locality of *C. brevipalmatus* which was repeated by Nabhitabhata et al. (2004) and Pauwels and Chan-ard (2006). Kaeng Krachen National Park is 85 km across continuous upland habitat south of the type locality of *C. rukhadeva* sp. nov. and based on data from Ulber (1993) and a photograph of a living specimen from Kaeng Krachen National Park (Fig. 9), this population shares with *C. rukhadeva* sp. nov. a yellow-orange iris; enlarged, unpaired, subcaudal scales; and a tail that is generally square in cross-section—character states that separate it from *C. brevipalmatus* (Table 4). Thus, although its species status remains uncertain, it is referred to here as *C.* cf. *rukhadeva* sp. nov. Chomdej et al. (2021) reported an undescribed species (sp. 9) in their phylogeny from Thong Pha Phum National Park, Thong Pha Phum District, Kanchanaburi Province, Thailand and government reports from Nabhitabhata et al. (2004) and Nabhitabhata and Chan-ard (2005) list *C. interdigitalis* from Huai Kha Khaeng, Uthai Province. These records have been repeated as both *C. brevipalmatus* and *C. interdigitalis* in a number of popular field and pocket guides and web sites on Thai reptiles. Based on the fact that all sequenced specimens from western Thailand north of the Isthmus of Kra are more closely related to *C. ngati* and *C.* cf. *interdigitalis* than they are to the sequenced specimen of *C. brevipalmatus* from its type locality in southern Thailand (Figs. 1 and 2), we hypothesize that none of specimens from the western Thailand are *C. interdigitalis* or *C. brevipalmatus* and that the Huai Kha Khaeng population may also be a new species.

The type locality of *Cyrtodactylus interdigitalis,* Tham Yai Nam Nao (Ulber 1993) occurs within the Nam Nao National Park that is part of an isolated upland massif in the eastern section of the Phetchabun Mountains. Within this upland region, *C. interdigitalis* has been reported from Tat Mak National Park (https://www.thainationalparks.com/species/cyrtodactylus-interdigitalis), Phu Kiew Wildlife Sanctuary (Chan-ard et al. 2015), and Phu

Kraden National Park (Chan-ard et al. 2015) ranging from ~700–1000 m in elevation (Fig. 1). Given that these are geographically proximate localities across continuous upland habitat we have no reason to believe at this point these populations are not conspecific.

The ND2 phylogenies (Fig. 2) were consistent with the CO1 phylogeny of Le et al. (2021) in that *Cyrtodactylus ngati* was recovered as the strongly supported sister species of their *C. interdigitalis* of unknown provenance. The ND2 trees recovered *C. brevipalmatus* and *C. elok* as sister species whereas the CO1 tree recovered *C. elok* as the sister species to the remaining *brevipalmatus* group. Although neither of these trees had strong nodal support for either topology, the sister group relationship was consistent with the strongly supported topology recovered in genus-wide analyses (Grismer et al. 2021a,b). Despite the low amount of uncorrected pairwise sequence divergence between *Cyrtodactylus ngati* and *C.* cf. *interdigitalis* (1.0–3.5%), *C. ngati* consistently plots as the most well-separated species in the multivariate analyses (Figs. 2, 3, and 5). We hypothesize that this difference in overall body shape may relate to a difference in microhabitat preference—as the type series was found on karst. However, *C. interdigitalis* has been reported to occur near karst formations and within cracks on a concrete bridge. The fact that the entire type series of *C. ngati* was found on limestone cliffs and in limestone crevices (Le et al. 2021) may represent the first transition of an arboreal species to a karst-dwelling species (Grismer et al. 2020, 2021b). It is becoming a well-established observation that karst-adapted species in gekkotans depart significantly in ecomorphology from their closely related non-karst-adapted species (Neilson and Oliver 2017; Grismer et al. 2020b; 2021c; Kaatz et al. 2021) as a result of different selection pressures on their morphology (Kaatz et al. 2021).

The discovery of *Cyrtodactylus rukhadeva* sp. nov. continues to underscore the unrealized herpetological diversity in the upland forests of the Tenasserim Mountains and that additional species have yet to be discovered—especially given that the borderlands between Thailand and Myanmar are renowned for their high degree of range-restricted endemism (Matsui 2006; Sumontha et al. 2012, 2017; Wilkinson et al. 2012; Connette et al. 2017; Grismer et al. 2017c; Matsui et al. 2018Mulcahy et al. 2018, Pawangkhanant et al. 2018; Suwannapoom et al. 2018; Lee et al. 2019). Additional field surveys followed up with appropriately conducted, statistically defensible integrative taxonomic analyses are necessary to continue increasing our understanding of this region's exceptional herpetofaunal diversity and endemism if we are to effectively initiate science-based conservation management programs.

Acknowledgements

We are thankful to the Laboratory Animal Research Center, University of Phayao and the Institute of Animal for Scientific Purposes Development (IAD), Thailand, for the permission to carry out field work (permit No. 610104022, issued to Chatmongkon Suwannapoom). Specimen collection protocols and animal use were approved by the Institutional Ethical Committee of Animal Experimentation of the University of Phayao, Phayao, Thailand (certificate number UP-AE61-01-04-0022 issued to Chatmongkon Suwannapoom). We also would like to express our gratitude to the Rabbit in the Moon foundation for help during the field work, and especially to Charnchai Bindusen and Juthamas Wangaryattawanich for organizing our fieldwork; and to Kawin Jiaranaisakul, Krarok Wohde, Torn Wohde, Jo Wohde, Maiday Ta-Au for assistance in the field; we thank Kanokwan Yimyoo for constant support and Vladislav A. Gorin, Pattarawhich Dawwrueng, Thiti Ruengsuwan, Akkrachai Aksornneam for help during the work in the field and in the lab. We thank Valentina F. Orlova (ZMMU, Russia) for support and letting us examine specimens under her care. We thank Bryan L. Stuart (NCSM) for the loan of specimens, photographs, and for generating and providing sequence data. Fieldwork, specimen collection, morphological examination, molecular phylogenetic analyses and data analyses for this paper were conducted with the financial support of the Russian Science Foundation (RSF grant No. 19-14-00050 to Nikolay A. Poyarkov); specimen collection and data analysis were also partially supported by the grants of the Unit of Excellence 2022 on Biodiversity and Natural Resources Management, University of Phayao (No. FF65-UoE003) to Chatmongkon Suwannapoom. The research was carried out within the frameworks of Russian State projects AAAA-A16116021660077-3 and AAAA-A17-117030310017-8, and partially supported by Moscow State University Grant for Leading Scientific Schools "Depository of the Living Systems" in frame of the MSU Development Program to Nikolay A. Poyarkov and Roman A. Nazarov.

References

Chan-ard T, Grossmann W, Gumprecht A, Schulz K-D (1999) Amphibians and Reptiles of Peninsular Malaysia And Thailand; An Illustrated Checklist. Bushmaster Publications, Würselen, 240 pp.

Chan-ard, T, Parr, JWK, Nabhitabhata, J. (2015) A Field Guide to the Reptiles of Thailand. Oxford University Press, New York, 214 pp. https://doi.org/10.1108/rr-03-2017-0074

Chomdej S, Pradit W, Suwannapoom C, Pawangkhanant P, Nganvongpanit K, Poyarkov NA, Che J, Gao Y, Gong S (2021) Phylogenetic analyses of distantly related clades of benttoed geckos (genus *Cyrtodactylus*) reveal an unprecedented amount of cryptic diversity in northern and western Thailand. Scientific Reports 11: 2328 https://doi.org/10.1038/s41598-020-70640-8

Connette GM, Oswald P, Thura MK, Connette KJL, Grindley ME, Songer M, Zug GR, Mulcahy DG (2017) Rapid forest clearing in a Myanmar proposed national park threatens two newly discovered species of geckos (Gekkonidae: *Cyrtodactylus*). PLoS One 12: e0174432. https://doi.org/10.1371/journal.pone.0174432

Cox MJ, van Dijk PP, Nabhitabhata J, Thirakhupt K (1998) A Photographic Guide to Snakes and Other Reptiles of Peninsular Malaysia, Singapore and Thailand. New Holland Publishers (UK) Ltd., London, 144 pp. https://doi.org/10.2307/1447416

Dring JCM (1979) Amphibians and reptiles from northern Trengganu, Malaysia, with descriptions of two new geckos: *Cnemaspis* and *Cyrtodactylus*. Bulletin of the British Museum (Natural History), Zoology 34: 181–24.

Ellis M, Pauwels OSG (2012) The bent-toed geckos (*Cyrtodactylus*) of the caves and karst of Thailand. Cave and Karst Science 39: 16–22.

Grismer LL (2008) On the distribution and identification of *Cyrtodactylus brevipalmatus* Smith, 1923 and *Cytodactylus elok* Dring, 1979. The Rafflels Bulletin of Zoology 56: 177–179.

Grismer LL (2011) Lizards of Peninsular Malaysia, Singapore and Their Adjacent Archipelagos. Edition Chimaira, Frankfurt am Main, 728 pp.

Grismer LL, Chan KO, Oaks JR, Neang T, Lang S, Murdoch ML, Stuart BL, Grismer JL (2020b) A new insular species of the *Cyrtodactylus intermedius* (Squamata: Gekkonidae) group from Cambodia with a discussion of habitat preference and ecomorphology. Zootaxa 4830: 75–102. https://doi.org/10.11646/zootaxa.4830.1.3

Grismer LL, Davis HR (2018) Phylogeny and biogeography of bent-toed geckos (*Cyrtodactylus* Gray) of the Sundaic swamp clade. Zootaxa 4472: 365–374. https://doi.org/10.11646/zootaxa.4472.2.9

Grismer, LL, Geissler P, Neang T, Hartmann T, Wagner P, Poyarkov NA (2021) Molecular phylogenetics, PCA, and MFA recover a new species of *Cyrtodactylus* (Squamata: Gekkonidae) from an isolated sandstone massif in northwestern Cambodia. Zootaxa 4949: 261–288. https://doi.org/10.11646/zootaxa.4949.2.3

Grismer LL, Ngo HN, Qi S, Ziegler T (2021) The phylogeny and taxonomy of *Goniurosaurus* (Squamata: Eublepharidae) and the correlation between habitat preference and ecomorphology in two species groups from karstic landscapes in northern Vietnam. Vertebrate Zoology 71: 335–352. https://doi.org/10.3897/Fvz.71.e65969

Grismer LL, Wood Jr PL, Aowphol A, Cota M, Grismer MS, Murdoch ML, Aguilar C, Grismer JL (2017) Out of Borneo, again and again: biogeography of the Stream Toad genus *Ansonia* Stoliczka (Anura: Bufonidae) and the discovery of the first limestone cave-dwelling species. Biological Journal of the Linnean Society. London 120: 371–395. https://doi.org/10.1111/bij.12886

Grismer LL, Wood Jr PL, Grismer MS, Quah ESH, Thura MK, Oaks JR, Lin A, Lim DY (2020a) Integrative taxonomic and geographic variation analyses in *Cyrtodactylus aequalis* (Squamata: Gekkonidae) from southern Myanmar (Burma): One species, two different stories. Israel Journal of Ecology and Evolution 66: 151–179. https://doi.org/10.1163/22244662-20191082

Grismer LL, Wood Jr PL, Le MD, Quah ESH, Grismer JG (2020) Evolution of habitat preference in 243 species of bent-toed geckos (Genus *Cyrtodactylus* Gray, 1827) with a discussion of karst habitat conservation. Ecology and Evolution 10: 13717–13730. https://doi.org/10.1002/ece3.6961

Grismer LL, Wood Jr PL, Poyarkov NA, Minh DL, Kraus F, Agarwal I, Oliver PM, Ngyuen S, Ngyuen T, Karunarathna S, Welton LJ, Stuart BL, Luu VK, Bauer AM, O'Connell KA, Quah ESH, Chan KO, Ngo H, Nazarov RA, Aowphol A, Chomdej S, Suwannapoom C, Siler CD, Anuar S, Tri NV, Grismer JL (2021a) Phylogenetic partitioning of the third-largest vertebrate genus in the world, *Cyrtodactylus* Gray, 1827 (Reptilia; Squamata; Gekkonidae) with a discussion on conservation and taxonomy. Vertebrate Zoology 71: 101–154. https://doi.org/10.3897/vertebrate-zoology.71.e59307

Grismer LL, Wood Jr PL, Poyarkov NA, Le MD, Karunarathna S, Chomdej S, Suwannapoom C, Qi S, Liu S, Che J, et al. (2021b) Karstic landscapes are foci of species diversity in the world's third-largest vertebrate genus *Cyrtodactylus* Gray, (Reptilia: Squamata; Gekkonidae). Diversity 13: 183. https://doi.org/10.3390/d13050183

Grismer LL, Wood PL, Quah ESH, Anuar S, Ngadi EB, Izam NAM, Ahmad N (2018) Systematics, ecomorphology, cryptic speciation and biogeography of the lizard genus *Tytthoscincus* Linkem, Diesmos & Brown (Squamata: Scincidae) from the sky-island archipelago of Peninsular Malaysia. Zoological Journal of the Linnean Society 183: 635–671. https://doi.org/10.1093/zoolinnean/zlx067

Grismer LL, Yushchenko PV, Pawangkhanant P, Naiduangchan M, Nazarov RA, Orlova VF, Suwannapoom C, Poyarkov NA. (2020) A new species of *Hemiphyllodactylus* Bleeker (Squamata; Gekkonidae) from Peninsular Thailand that converges in morphology and color pattern on *Pseudogekko smaragdinus* (Taylor) from the Philippines. Zootaxa 4816 2: 171–190. https://doi.org/10.11646/zootaxa.4816.2.2

Hoang DT, Chernomor O, von Haeseler A, Minh BQ, Vinh LS (2018) UFBoot2: Improving the ultrafast bootstrap approximation. Molecular Biology and Evolution 35: 518–522. https://doi.org/10.1093/molbev/msx281

Huelsenbeck JP, Ronquist F, Nielsen R, Bollback J.P (2001) Bayesian Inference of phylogeny and its impact on evolutionary biology. Science 294: 2310–2314. https://doi.org/10.1126/science.1065889

Jombart T, Collins C (2015) A tutorial for discriminant analysis of principal components (DAPC) using adegenet 2.0.0. Available at: http://adegenet.r-forge.r-project.org/files/tutorial-dapc-pdf

Jombart T, Devillard S, Balloux F (2010) Discriminant analysis of principal components: a new method for the analysis of genetically structured populations. BMC Genetics 11: 94. https://doi.org/10.1186/1471-2156-11-94

Kaatz A, Grismer JL, Grismer LL (2021) Convergent evolution of karst habitat preference and its ecomorphological correlation in three species of bent-toed geckos (*Cyrtodactylus*) from Peninsular Malaysia. Vertebrate Zoology 71: 367–386. https://doi.org/10.3897/vz.71.e66871

Kalyaanamoorthy S, Minh BQ, Wong TK, von Haeseler A, Jermiin LS (2017) ModelFinder: fast model selection for accurate phylogenetic estimates. Nature Methods 14: 587. https://doi.org/10.1038/nmeth.4285

Kumar S, Stecher G, Tamura K (2016) MEGA7: Molecular evolutionary genetics analysis version 7.0 for bigger datasets. Molecular Biology and Evolution 33: 1870–1874. https://doi.org/10.1093/molbev/msw054

Le DT, Sitthivong S, Tran TT, Grismer LL, Truong QN, Le MD, Ziegler T, Luu VQ (2021) First record of the *Cyrtodactylus brevipalmatus* group (Squamata: Gekkonidae) from Vietnam with description of a new species. Zootaxa 4969: 492–510.

Lee JL, Miller AH, Zug GR, Mulcahy DG (2019) The discovery of Rock Geckos *Cnemaspis* Strauch, 1887 (Squamata: Gekkonidae) in the Tanintharyi Region, Myanmar with the description of two new species. Zootaxa, 4661: 40–64.

Lleonart J, Salat J, Torres GJ (2000) Removing allometric effects of body size in morphological analysis. Journal of Theoretical Biology 205: 85–93. https://doi.org/10.1006/jtbi.2000.2043

Macey JR, Larson A, Ananjeva NB, Fang Z, Papenfuss, TJ (1997) Two novel gene orders and the role of light-strand replication in rearrangement of the vertebrate mitochondrial genome. Molecular Biology and Evolution 14: 91–104. https://doi.org/10.1093/oxfordjournals.molbev.a025706

Manthey U, Grossmann W (1997) Ambphibien and Reptilien Südostasiens. Natur und Tier Verlag, Münster, 512 pp.

Matsui M. (2006) Three new species of *Leptolalax* from Thailand (Amphibia, Anura, Megophryidae). Zoological Science 23: 821–830. https://doi.org/10.2108/zsj.23.821

Miller MA, Pfeiffer W, Schwartz T (2010) Creating the CIPRES Science Gateway for inference of large phylogenetic trees. In: Gate-

way Computing Environments Workshop (GCE), New Orleans (USA), November 2010, IEEE, 1–8. https://doi.org/10.1109/GCE.2010.5676129

Minh BQ, Nguyen MAT, von Haeseler A (2013) Ultrafast approximation for phylogenetic bootstrap. Molecular Biology and Evolution 30: 1188–1195. https://doi.org/10.1093/molbev/mst024

Mulcahy DG, Lee JL, Miller AH, Chand M, Thura MK, Zug GR (2018) Filling the BINs of life: report of an amphibian and reptile survey of the Tanintharyi (Tenasserim) Region of Myanmar, with DNA barcode data. ZooKeys 757: 85–152. https://doi.org/10.3897/zookeys.757.24453

Murdoch ML, Grismer LL, Wood Jr PL, Neang T, Poyarkov NA, Tri NV, Nazarov RA, Aowphol A, Pauwels OSG, Nguyen HN, Grismer JL (2019) Six new species of the *Cyrtodactylus intermedius* complex (Squamata: Gekkonidae) from the Cardamom Mountains and associated highlands of Southeast Asia. Zootaxa 4554: 1–62. https://doi.org/10.11646/zootaxa.4554.1.1

Nabhitabhata J, Chan-ard T, Chuaynkern Y (2004). Checklist of Amphibians and Reptiles in Thailand. Office of Environmental Policy and Planning, Bangkok. 152pp.

Nabhitabhata J, Chan-ard T (2005) Thailand Red Data: Mammals, Reptiles and Amphibians. Office of Natural Resources and Environmental Policy and Planning (Biodiversity Series 14), Bangkok, 180pp.

Nguyen L-T, Schmidt HA, von Haeseler A, Minh BQ (2015). IQ-TREE: A fast and effective stochastic algorithm for estimating maximum likelihood phylogenies. Molecular Biology and Evolution 32: 268–274. https://doi.org/10.1093/molbev/msu300

Nielsen SV, Oliver PM (2017) Morphological and genetic evidence for a new karst specialist lizard from New Guinea (*Cyrtodactylus*: Gekkonidae). Royal Society Open Science 4: 170781. https://doi.org/10.1098/rsos.170781

Pauwels OSG, Chan-ard T (2006) Reptiles of Kaeng Krachan National Park, western Thailand. Natural History Bulletin of the Siam Society 54: 89–108.

Pawangkhanant P, Poyarkov NA, Duong TV, Naiduangchan M, Suwannapoom C (2018) A new species of *Leptobrachium* (Anura, Megophryidae) from western Thailand. PeerJ 6: e5584. https://doi.org/10.7717/peerj.5584

R Core Team. (2018) R: A language and environment for statistical computing. R Foundation for Statistical Computing. Vienna. Available from: http://www.R-project.org (accessed 29 December 2018)

Rambaut A, Drummond AJ, Xie D, Baele G, Suchard MA (2018) Posterior summarization in Bayesian phylogenetics using Tracer v1.7. Systematic Biology 67: 901–904. http://doi.org/10.1093/sysbio/syy032

Reist JD (1986) An empirical evaluation of coefficients used in residual and allometric adjustment of size covariation. Canadian Journal of Zoology 64: 1363–1368. https://doi.org/10.1139/z86-203

Ronquist F, Teslenko M, van der Mark P, Ayres DL, Darling A, Höhna S, Larget B, Liu L, Suchard MA, Huelsenbeck JP (2012) MrBayes 3.2: efficient Bayesian phylogenetic inference and model choice across a large model space. Systematic Biology 61: 539–542. http://doi.org/10.1093/sysbio/sys029

Smith MA (1923) Notes on reptiles and batrachians from Siam and Indo-China (No. 2). Journal of Natural History Society of Siam 6: 47–53.

Smith MA (1930) The reptilia and amphibia of the Malay Peninsula from the Isthmus of Kra to Singapore including the adjacent islands. Bulletin of the Raffles Museum 3: 1–135. https://doi.org/10.1080/00222933008673247

Smith MA (1935) The fauna of British India, including Ceylon and Burma. Reptiles and Amphibia. Vol. II. Sauria. Taylor and Francis, London, 440 pp.

Stuart B (1999) Amphibians and Reptiles. In: Duckworth JW, Salter RE, Khounboline K (Eds.) Wildlife in Lao PRD: 1999 Status Report. Vientiane, IUCN – The World Conservation Union – Wildlife Conservation Society – Centre for Protected Areas and Watershed Management, 43–67.

Sumontha M, Kunya K, Dangsri S, Pauwels OSG (2017) *Oligodon saiyok*, a new limestone dwelling kukri snake (Serpentes: Colubridae) from Kanchanaburi Province, western Thailand. Zootaxa 4294: 316–328. https://doi.org/10.11646/zootaxa.4294.3.2

Sumontha M, Pauwels OSG, Kunya K, Limlikhitaksorn C, Ruksue S, Taokratok A, Ansermet M, Chanhome L (2012) A new species of Parachute Gecko (Squamata: Gekkonidae: genus *Ptychozoon*) from Kaeng Krachan National Park, western Thailand. Zootaxa 3513: 68–78.

Suwannapoom C, Sumontha M, Tunprasert J, Ruangsuwan T, Pawangkhanant P, Korost DV, Poyarkov NA (2018) A striking new genus and species of cave-dwelling frog (Amphibia: Anura: Microhylidae: Asterophryinae) from Thailand. PeerJ 6: e4422. https://doi.org/10.7717/peerj.4422

Taylor EH (1963) The lizards of Thailand. The University of Kansas Science Bulletin 44: 687–1077.

Thorpe RS (1975) Quantitative handling of characters useful in snake systematics with particular reference to intraspecific variation in the Ringed Snake *Natrix natrix* (L.). Biological Journal of the Linnean Society 7: 27–43. https://doi.org/10.1111/j.10958312.1975.tb00732.x

Thorpe RS (1983) A review of the numerical methods for recognising and analysing racial differentiation. In: Felsenstein J, ed. Numerical Taxonomy. NATO ASI Series (Series G: Ecological Sciences), vol. 1. Springer-Verlag, Berlin, 404–423. https://doi.org/10.1007/978-3-642-69024-2_43

Trifinopoulos J, Nguyen L-T, von Haeseler A Minh BQ (2016) W-IQ-TREE: a fast online phylogenetic tool for maximum likelihood analysis. Nucleic Acids Research 44: W232-W235. https://doi.org/10.1093/nar/gkw256

Turan C (1999) A note on the examination of morphometric differentiation among fish populations: The truss system. Turkish Journal of Zoology 23: 259–263.

Ulber T (1993) Bemerkungen über cyrtodactyline Geckos aus Thailand nebst Beschreibungen von zwei neuen Arten (Reptilia: Gekkonidae). Mitteilungen aus dem Zoologischen Museum in Berlin 69: 187–200. https://doi.org/10.1002/mmnz.4840690202

Welch, KR, Cooke PS, Wright AS (1990) Lizards of the Orient: A Checklist. Robert E. Krieger Publishing Company, Malabar, Florida, 372 pp.

Wilkinson JA, Sellas AB, Vindum JV (2012) A new species of *Ansonia* (Anura: Bufonidae) from northern Tanintharyi Division, Myanmar. Zootaxa 3163: 54–68.